

Alloys and Compounds

Elsevier Editorial System(tm) for Journal of
Manuscript Draft

Manuscript Number: JALCOM-D-19-05063R2

Title: Conventional and inverse barocaloric effects in ferroelectric
NH₄HSO₄

Article Type: Full Length Article

Keywords: Polymorphic phase transformation, Phase diagram,
Order-disorder phenomena, Entropy, Barocaloric effect

Corresponding Author: Professor Igor Flerov,

Corresponding Author's Institution: Kirensky Institute of Physics

First Author: Igor Flerov

Order of Authors: Igor Flerov; Mikhail Gorev; Ekaterina Mikhaleva;
Evgeniy Bogdanov

Abstract: In this study, the conventional and inverse barocaloric effects (BCE) in ferroelectric NH₄HSO₄ are reported. Maximum extensive and intensive BCE near order-disorder phase transition can be achieved at low pressure $p \leq 0.1$ GPa. Large thermal expansion of the crystal lattice plays a very important role in the developing conventional BCE and conversation between BCE of different sign in the narrow temperature range.

Dear Editor,

Consider please our manuscript, devoted to some new results obtained during the study of the intensive and extensive barocaloric effects near phase transitions in ferroelectric NH_4HSO_4 .

We hope that the results will be of interest to readers of Journal of Alloys and Compounds.

Sincerely Yours,

Prof. Igor Flerov

Conventional and inverse barocaloric effects in ferroelectric NH_4HSO_4

Mikhail V. Gorev, Ekaterina A. Mikhaleva, Igor N. Flerov, Evgeniy V. Bogdanov

e-mail: gorev@iph.krasn.ru (M.V. Gorev), katerina@iph.krasn.ru (E.A. Mikhaleva),
flerov@iph.krasn.ru (I.N. Flerov), evbogdanov@yandex.ru (E.V. Bogdanov)

Abstract

In this study, the conventional and inverse barocaloric effects (BCE) in ferroelectric NH_4HSO_4 are reported. Maximum extensive and intensive BCE near order-disorder phase transition can be achieved at low pressure $p \leq 0.1$ GPa. Large thermal expansion of the crystal lattice plays a very important role in the developing conventional BCE and conversation between BCE of different sign in the narrow temperature range.

Prime Novelty Statement

Detailed studies of the barocaloric effect at the phase transitions $P2_1/c(T1) \leftrightarrow Pc(T2) \leftrightarrow P1$ in ammonium hydrosulphate were carried out for the first time and showed new peculiar properties of NH_4HSO_4 .

- 1) Both ferroelectric transformations are characterized by large baric coefficients of different sign.
- 2) Hydrostatic pressure strongly decreases the entropy jump at $T2$ which reaches zero at a pressure of 0.17 GPa.
- 3) Very low pressure is needed to realize the maximum values of the extensive and intensive inverse BCE at $T2$.
- 4) Large thermal expansion of the crystal lattice leads to two very important points. Firstly, the conventional BCE at $T1$ can be greatly increased to values much higher than the magnitudes corresponding to the entropy of the phase transition. Secondly, in the case of the negative baric coefficient at $T2$, a conversion from the inverse to conventional BCE can be realized by low pressure in the narrow temperature range.
- 5) The results obtained are very important and promising from the point of view of searching materials with large barocaloric effects and designing original cooling cycles.

Response to Reviewers

To Reviewer #1:

Dear Sir/Madam,

Thank you very much for the efficient comments and appreciation of our paper.

Q1. The final refinement convergence (R_p and R_{Wp}) should be given.

OK! We added this information to the description of X-ray structural characterization (page 4):

Instead of

“Fig. 1 shows the results of Rietveld refinement”

we put

“Fig. 1 shows the results of Rietveld refinement ($R_{wp} = 6.04$, $R_p = 4.23$, $\chi^2 = 2.06$).”

Q2. In figure 4, the maximum barocaloric entropy changed slightly, and the peak shifted to low temperature. It seems that the pressure-dependent entropy change near T_1 that arises on heating through the first order phase transition.

However, first order phase transition usually exhibits large thermal hysteresis.

How about the pressure-dependent entropy change near T_1 on cooling?

Sorry, we think that you mean the transition at T_2 .

Unfortunately, experimental setups (adiabatic calorimeter and DTA under pressure) do not allow measurements in cooling mode. Therefore, the determination of the BCE was carried out only in the heating mode. The hysteresis of the phase transition temperature $\delta T_2 \leq 2.5$ K [Izvestiya AN USSR, 39 (1975) 752-757] is much smaller than temperature interval of BCE at $p > 0.02$ GPa.

In addition, it's hard to get the maximum adiabatic temperature values, especially under low hydrostatic pressure. Therefore, adiabatic temperature changes between 140 K and 170 K under different hydrostatic pressure should be inset in figure 4b.

OK! We changed the Figure 4b by adding an insert.

Q3. Coexistence of the conventional and inverse barocaloric effects in one material is very intriguing. The negative barocaloric effect may propose novel combinations with conventional (positive) barocaloric effect to further enhance the cooling efficiency. Similar approach has been proposed in electrocaloric materials

to enhance the coefficient of performance (COP) by combining conventional (positive) and inverse (negative) electrocaloric effects together [Nano Energy (2015) 16, 419]. Is it possible to enhance the COP by combining conventional and inverse barocaloric effects? If it is possible, what is the original cooling cycles?

You are absolutely right. Coexistence of the conventional and inverse barocaloric effects in one material is very intriguing. However, in the case of NH_4HSO_4 , these effects associated with two transitions are too far in temperature (160 and 270 K). In the region near 160 K, the conventional effect due to the change in the entropy of the lattice under pressure is rather small. In our opinion, a more interesting phenomenon can be associated with direct and inverse effects observed at a single transition under the action of uniaxial stresses along different crystallographic axes. We are currently working in this direction. We hope that the results of such studies will be more informative for the analysis of COP.

Thank your for the reference on interesting paper. We know it and will use further./

Q4. "This paper demonstrates BCE in NH_4HSO_4 undergoing two successive ferroelectric phase transitions of displacive and order/disorder type at T_1 and at T_2 , respectively. Both transformations are characterized by large baric coefficients of different sign." This conclusion is not clear. It has been shown that the purely displacive and order-disorder (OD) cases are merely limiting situations, but they are typically thought to describe a majority of the known ferroelectric phase transitions. In the displacive structural phase transformation case, atoms remain associated with their average positions, and phase transition occurs as the positional pattern changes its symmetry. If the corresponding phonon mode frequency decreases to zero near the phase transition temperature, it is a signature of a displacive case (known as soft mode behavior). In the OD case, the structural model involves partially occupied sites, and the transition occurs as the symmetry of the occupational distribution is broken. As a result, the relevant phonon frequency stays temperature independent, while another strongly temperature dependent excitation of the relaxation type occurs. More discussion in the main text or additional experiments should be provided.

Thank you for your comments. Indeed, the mechanism of the structural phase transitions is very often complicated and sometimes can even include the features of both displacive and OD cases. On the other hand, it is known that the entropy as a quantitative characteristic is strongly different for transformations of both types. This situation is observed in the case of NH_4HSO_4 : $\Delta S_1 \ll \Delta S_2$. However, we

decided not to discuss such a complex issue, which is not directly related to our research, and make some changes in Conclusions.

Instead of

"This paper demonstrates BCE in NH_4HSO_4 undergoing two successive ferroelectric phase transitions of displacive and order/disorder type at T_1 and at T_2 , respectively. Both transformations are characterized by large baric coefficients of different sign."

we put

"This paper demonstrates BCE in NH_4HSO_4 undergoing two successive ferroelectric phase transitions characterized by significantly different entropy changes ($\Delta S_1=1.2 \text{ J/mol}\cdot\text{K}$, $\Delta S_2=7.6 \text{ J/mol}\cdot\text{K}$) and large baric coefficients of different sign ($dT_1/dp=+90 \text{ K/GPa}$ and $dT_2/dp=-123 \text{ K/GPa}$)."

To Reviewer #2

Dear Sir/Madam,

Thank you very much for your comments, questions and appreciation of our paper.

1. What is the mechanism underlying the observation of the inverse barocaloric effects?

Both extensive ΔS_{BCE} and intensive ΔT_{AD} barocaloric parameters strongly depend on the volume thermal expansion $(\partial V/\partial T)_p$ which very often shows large change near the temperature of the phase transitions. In accordance with Eq. 1, the negative baric coefficient dT/dp associated with the negative value $(\partial V/\partial T)_p$ is the reason of the inverse BCE at T_2 accompanied by increase in entropy and decrease in temperature under pressure increase.

2. Why do the inverse barocaloric effects coexist with the conventional barocaloric effects?

Conventional (near T_1) and inverse (near T_2) BCE are observed at different phase transitions and determined by the sign of the temperature shift of these transitions under pressure: $dT_1/dp>0$, $dT_2/dp<0$ (Fig. 2).

Near 160 K these effects are associated with different components - with the change in the entropy of the crystal lattice (conventional) and the change in anomalous entropy (inverse, $dT_2/dp<0$).

3. The maximum barocaloric effects were observed near the order-disorder phase transition temperature, where the heat capacity C_p should also reach the maximum value. It would be better if the authors could measure heat capacity at various temperatures.

The detailed heat capacity studies at $p=0$ was performed by us earlier in wide temperature range [19], where both the lattice and anomalous components of heat capacity and entropy were determined. Using these data, the values of barocaloric effects were determined at the first stage (Fig. 3-4 (a, b)). At the second stage, we took into account the dependence of the entropy of the crystal lattice on pressure using the data on thermal expansion (Fig. 4 (c, d)). And finally, using the DTA data under pressure, we were able to take into account the pressure dependence of the entropy jump at the first-order phase transition at T_2 (Fig. 5).

4. The authors might discuss the potential application of the coexistence of the inverse barocaloric effect and the conventional barocaloric effect. An idea has been proposed to improve the cooling efficiency in ferroelectrics via combining inverse (negative) and conventional (positive) electrocaloric effects [Nano Energy 16, 419-427 (2015)].

Thank your for the reference on interesting paper. We know it and will use in our further researches.

You are absolutely right. Coexistence of the conventional and inverse barocaloric effects in one material is very intriguing. However, in the case of NH_4HSO_4 , these effects associated with two transitions are too far in temperature (160 and 270 K). In the region near 160 K, the conventional effect due to the change in the entropy of the lattice under pressure is rather small. In our opinion, a more interesting phenomenon can be associated with direct and inverse effects observed at a single transition under the action of uniaxial stresses along different crystallographic axes. We are currently working in this direction. We hope that the results of such studies will be more informative for the analysis of COP.

Thank you again.

Best regards,

Igor Flerov.

Response to Reviewers

To Reviewer #1:

Dear Sir/Madam

Thank you very much for your positive final decision on our paper.

Best regards,
Igor Flerov.

To Reviewer #3:

Dear Sir/Madam

Thank you very much for your positive final decision on our paper.

Best regards,
Igor Flerov.

To Reviewer #4:

Dear Sir/Madam,

Thank you for your interesting question on lattice constants change with pressure and temperature.

Indeed, such information would be useful in our analysis of BCE.

Unfortunately, firstly, such data are not available in the literature and, secondly, we were not able to perform such studies due to the lack of appropriate equipment.

On the other hand, we took into account the data on the behaviour of lattice constants of related $(\text{NH}_4)_2\text{SO}_4$ [15] where no noticeable effect of pressure on the thermal expansion of the lattice was found.

Please see page 8 in the manuscript:

“Taken into account the data of the thermal expansion study of the related $(\text{NH}_4)_2\text{SO}_4$ [15], it was suggested that the values of β_{LAT} and V_m of NH_4HSO_4 are also weakly depend on the pressure.”

In connection with the above, we did not make any corrections and/or additions in the text of the manuscript.

Thank you very much for your positive final decision on our paper.

Best regards,
Igor Flerov.

Conventional and inverse barocaloric effects in ferroelectric NH_4HSO_4

Mikhail V. Gorev^{a,b}, Ekaterina A. Mikhaleva^{a,b}, Igor N. Flerov^{a,b,*}, Evgeniy V. Bogdanov^{a,c}

^a*Kirensky Institute of Physics, Federal Research Center KSC SB RAS, Krasnoyarsk, Russia*

^b*Institute of Engineering Physics and Radioelectronics, Siberian Federal University, Krasnoyarsk, Russia*

^c*Institute of Engineering Systems and Energy, Krasnoyarsk State Agrarian University, 660049 Krasnoyarsk, Russia*

Abstract

In this study, the conventional and inverse barocaloric effects (BCE) in ferroelectric NH_4HSO_4 are reported. Maximum extensive and intensive BCE near order–disorder phase transition can be achieved at low pressure $p \leq 0.1$ GPa. Large thermal expansion of the crystal lattice plays a very important role in the developing conventional BCE and conversation between BCE of different sign in the narrow temperature range.

Keywords: Polymorphic phase transformation, Phase diagram, Order–disorder phenomena, Entropy, Barocaloric effect

PACS: 62.50.-p, 65.40.-b, 81.30.-t

1. Introduction

In recent years, much attention is paid to caloric effects (CE) in solids, particularly in ferroics, associated with the reversible change in the temperature, ΔT_{AD} , or entropy, ΔS_{CE} , under variation of the external field in adiabatic and isothermal conditions, respectively [1, 2, 3, 4]. One of the main reasons for this interest is related to the possibility to use the materials showing large CE's

*Corresponding author

Email addresses: gorev@iph.krasn.ru (Mikhail V. Gorev), katerina@iph.krasn.ru (Ekaterina A. Mikhaleva), flerov@iph.krasn.ru (Igor N. Flerov), evbogdanov@iph.krasn.ru (Evgeniy V. Bogdanov)

as solid state refrigerants in alternative cooling cycles [5, 6, 7, 8]. Among the CEs of different physical nature, the barocaloric effect (BCE) is distinguished by a serious advantage associated with its universality. Indeed, both extensive ΔS_{BCE} and intensive ΔT_{AD} barocaloric parameters strongly depend on the volume thermal expansion $(\partial V/\partial T)_p$ which very often shows large change near the temperature of any phase transitions: ferroelectric, ferroelastic, ferromagnetic

$$\Delta S_{BCE} = - \int_0^p \left(\frac{\partial V}{\partial T} \right)_p dp, \quad \Delta T_{AD} = - \frac{T}{C_p} \Delta S_{BCE}, \quad (1)$$

where C_p is the heat capacity.

The most intensively, BCE was studied in materials undergoing ferroelastic [9, 10] and ferromagnetic [11, 12, 13, 14] phase transitions. As to the ferro-
 5 electrics, their barocaloric efficiency was investigated only sporadically [11, 15, 16, 17]. It is known that the values and behavior of the BCE depend on the behavior and change in the entropy ΔS of the phase transition as well as on the sensitivity of the phase transition temperature to hydrostatic pressure [9, 10]. Thus, ferroics undergoing order–disorder transformations accompanied by large
 10 change in the volume and as result in baric coefficient, $dT_0/dp = \delta V/\delta S$, are the most promising barocaloric materials. Important requirements for caloric materials are also their low cost and ecological tolerance.

It has recently been shown that ferrielectric $(\text{NH}_4)_2\text{SO}_4$ meets all of the above requirements [15]. Due to significant values of $\Delta S=17 \text{ J/mol}\cdot\text{K} \approx R \ln 8$
 15 and $dT_0/dp=-45 \text{ K/GPa}$, rather large extensive and intensive BCE were observed in the region of the phase transition $Pnam - Pna2_1$ under low pressure. In accordance with Eq. 1, the negative baric coefficient associated with the negative value $(\partial V/\partial T)_p$ is the reason of the inverse BCE_{inv} in $(\text{NH}_4)_2\text{SO}_4$ accompanied by increase/decrease in entropy/temperature under pressure in-
 20 crease. It was also found that large coefficient of the volume thermal expansion of the crystal lattice, β_{LAT} , can play an important role in formation of real BCE in material. Indeed, in the case of ammonium sulphate, large positive value $\beta_{LAT} = 1.4 \times 10^{-4} \text{ K}^{-1}$ leads to decrease in the inverse BCE_{inv} under pressure due to the appearance of the conventional contribution BCE ($\Delta S_{BCE} < 0$,

$\Delta T_{AD} > 0$) [15]. The conversion from BCE_{inv} to BCE_{conv} was observed in a narrow temperature range. When pressure increases, the ratio between these values changes and at $p=0.25$ GPa is about $BCE_{conv}/BCE_{inv}=0.15$. Thus, to get correct information on BCE in materials with large thermal expansion coefficient, it is necessary to take into account the effect of pressure on the lattice entropy. It is obvious that the magnitude of baric coefficient strongly effects on the maximum value of the intensive BCE [18]. In this respect, it is interesting to analyze both BCE in material with anomalously large negative or positive dT/dp . From this point of view, another ferroelectric crystal, ammonium hydrogen sulphate, is very good example.

Indeed, NH_4HSO_4 undergoes two successive phase transitions $P2_1/c \leftrightarrow Pc \leftrightarrow P1$, of the strong second and first order at $T_1=271$ K and $T_2=159$ K, respectively. One more difference is that anomaly of volumetric thermal expansion coefficient is positive at T_1 and negative at T_2 [19] which leads to BCE_{conv} and BCE_{inv} . Thus, the contribution from the thermal expansion of the crystal lattice to both BCE will be also different. Despite the large difference in the entropy of the phase transitions ($\Delta S_1=1.2$ J/mol·K, $\Delta S_2=7.6$ J/mol·K), one can suppose that BCE_{conv} at T_1 could be strongly increased due to rather large value of $\beta_{LAT}=2 \times 10^{-4}$ K $^{-1}$ far from the phase transition points. In addition, like $(NH_4)_2SO_4$, ammonium hydrogen sulphate is also easy to prepare, cheap and environmentally friendly.

In the present paper, we performed an analysis of extensive and intensive barocaloric efficiency of NH_4HSO_4 near both phase transformations based on methods developed by us earlier [18]. For this aim, the dependencies of $\Delta T_{AD}(T, p)$ and $\Delta S_{BCE}(T, p)$ were determined using data on total and anomalous heat capacity [19], the $T-p$ phase diagram and the dependencies of entropy of the phase transitions on temperature and pressure.

2. Experimental details

Powder samples of ammonium hydrogen sulphate were obtained by slow evaporation at 45°C from an aqueous solution containing equimolar quantities
55 of high purity raw materials $(\text{NH}_4)_2\text{SO}_4$ and H_2SO_4 .

The quality of samples used for the experiments was checked at room temperature using XRD, which revealed a monoclinic symmetry consistent with the space group $P2_1/c$ ($Z=8$) suggested in Refs. [20, 21]. No additional phases were observed in the samples. Fig. 1 shows the results of Rietveld refinement
60 ($R_{wp}=6.04$, $R_p=4.23$, $\chi^2=2.06$). The unit cell parameters $a = 24.770(6)\text{\AA}$, $b = 4.611(1)\text{\AA}$, $c = 14.871(4)\text{\AA}$, $\beta = 89.70(1)$ grad are consistent with the values determined in Ref. [21].

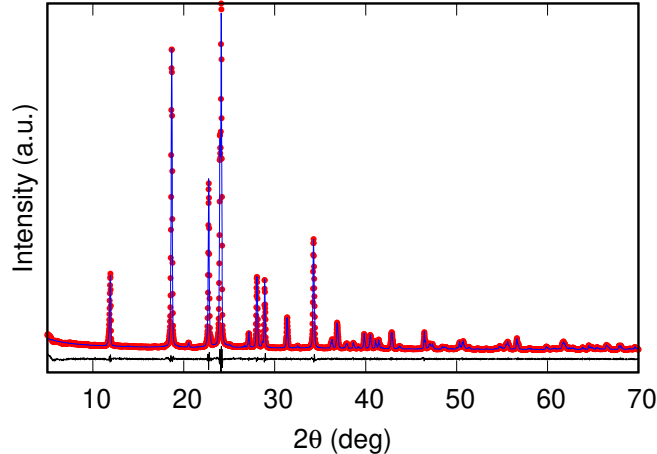


Figure 1: Difference Rietveld plot for NH_4HSO_4 at room temperature.

Quasi-ceramic samples of NH_4HSO_4 in the form of disks, approximately 1.0 mm thick and approximately 6 mm in diameter, were used for investigations.
65 Because of the presence of ammonium ion in crystal, the heat treatments of ceramics were not performed. For dielectric measurements, electrodes on pellets were formed by conducting glue covered the opposite sides of the sample.

The effect of hydrostatic pressure on temperature and entropy of the phase transitions was studied using a piston-cylinder type vessel associated with a

70 pressure multiplier. Pressure of up to 0.25 GPa was generated using a mixture
of silicon oil and pentane exhibiting optimal electrical and heat conductivity,
solidification point and viscosity as the pressure-transmitting medium. Pressure
and temperature were measured using a manganin resistive sensor and a copper-
constantan thermocouple, with accuracies of about $\pm 10^{-3}$ GPa and ± 0.3 K
75 respectively.

The dependencies $T_1(p)$ and $T_2(p)$ were revealed, firstly, in experiments with
differential thermal analysis (DTA) and, secondly, by measurements of the per-
mittivity ε . In the former case, to detect anomalies of DTA-signal associated
with the heat capacity anomalies, high-sensitive differential copper-germanium
80 thermocouple was used. In the latter case, experiments were performed using
an E7-20 immittance meter. To ensure the reliability of the results, the mea-
surements were performed for both increasing and decreasing pressure cycles.

3. Results and discussion

At ambient pressure, the anomalies of DTA signal and ε were detected at
85 about $T_1 = 271.5 \pm 1.0$ K and $T_2 = 160 \pm 2$ K (Fig. 2 (a) and (b)), which agree well
with values observed during measurements of the heat capacity [19]. Fig. 2(c)
shows that an increase in pressure leads to linear increase and decrease in T_1 and
 T_2 , respectively: $dT_1/dp = +90 \pm 15$ K/GPa and $dT_2/dp = -123 \pm 15$ K/GPa
which are significantly higher than that for ammonium sulfate [15].

90 Due to the limited sensitivity of the DTA method, the area under the DTA
peak at T_2 represents a change in the enthalpy δH_2 (entropy $\delta S_2 = \delta H_2/T_2$)
jump at the first order phase transition $Pc \leftrightarrow P1$ in NH_4HSO_4 . An increase in
pressure is accompanied by a linear decrease in the value of δS_2 which reaches
zero at $p \approx 0.17$ GPa (Fig. 2(d)) that can be considered as corresponding to the
95 pressure of the tricritical point. On the other hand, it is unlikely that such a low
pressure may affect the degree of disordering of structural elements in phases
 $P2_1/c$ and Pc , and as a result the total entropy change at the $Pc \leftrightarrow P1$ trans-
formation, $\Delta S_2(p) = \delta S_2(p) + \Delta S_2^*(T, p)$, remains constant. Here $\Delta S_2^*(T, p)$ is

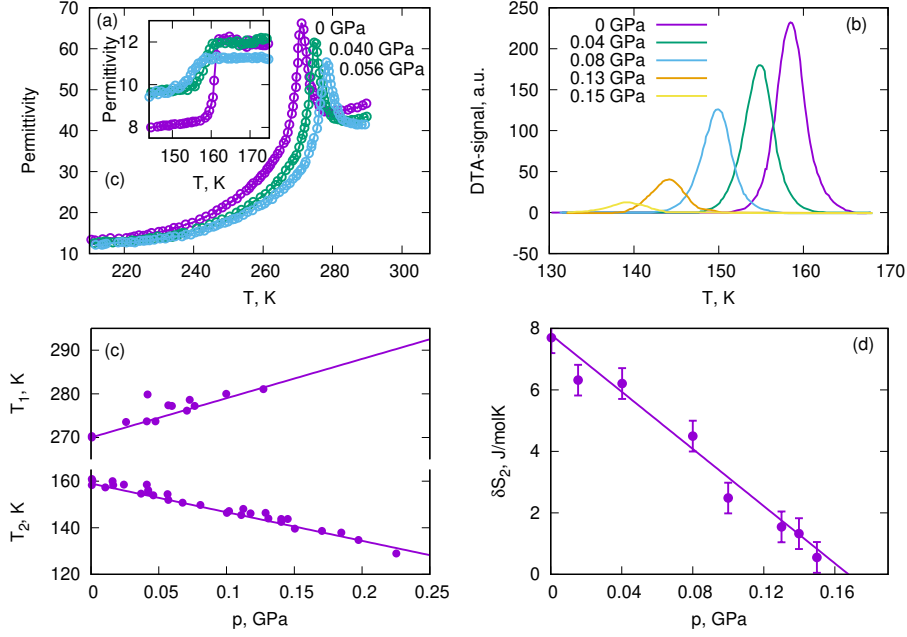


Figure 2: (a) Temperature dependencies of permittivity for NH_4HSO_4 around T_1 and T_2 and (b) anomalous component of the DTA signal near T_2 at different hydrostatic pressure. (c) Temperature – pressure phase diagram combining the results on the DTA signal and permittivity study. (d) Entropy jump δS_2 for the first-order transition in NH_4HSO_4 at different hydrostatic pressure.

the temperature- and pressure-dependent contribution.

100 The analysis of extensive and intensive BCE in NH_4HSO_4 was performed in three steps.

At the first stage, the possible influence of pressure on the entropy of the crystal lattice ΔS_{LAT} was not taken into account. Fig. 3 demonstrates the temperature behavior of the lattice $S_{LAT}(T) - S_{LAT}(100 \text{ K}) = \int_{100}^T (C_{LAT}/T) dT$ and total $S = \int_{100}^T (C_p/T) dT$ entropies in the vicinities of T_1 and T_2 . Temperature dependencies $S(T)$ under pressure were determined by summation of the lattice entropy S_{LAT} and the anomalous contributions ΔS_1 and ΔS_2 shifted along the temperature scale in accordance with the sign of baric coefficients dT_1/dp and dT_2/dp . The values and behavior of extensive BCE, ΔS_{BCE} , at
110 different pressure were determined from temperature dependencies of the total

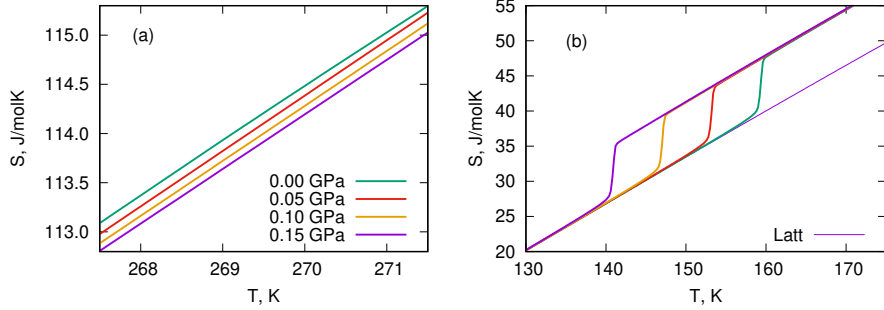


Figure 3: Temperature dependencies of total entropy of NH_4HSO_4 at different hydrostatic pressure near (a) T_1 and (b) T_2 .

entropy as a difference $\Delta S_{BCE} = S(T, p) - S(T, p = 0)$ at constant temperature (Fig. 4(a)). The temperature dependencies of the intensive BCE were revealed analyzing plots of $S(T, p) = S_{LAT}(T, p = 0) + \Delta S(T, p)$ at constant entropy $S(T, p) = S(T + \Delta T_{AD}, p = 0)$ (Fig. 4(b)). Large difference in BCE at T_1 and T_2 at the same pressure is the result of the different values of ΔS_1 and ΔS_2 .

It is known [22] that if we neglect the contribution of the thermal expansion of the crystal lattice, the maximum values of both BCE are limited by the value of the entropy of the phase transition: $(\Delta S_{BCE}^{max})_{T_1} = \Delta S_1 = -10 \text{ J/kg}\cdot\text{K}$, $(\Delta T_{AD}^{max})_{T_1} = 2 \text{ K}$; $(\Delta S_{BCE}^{max})_{T_2} = \Delta S_2 = 68 \text{ J/kg}\cdot\text{K}$, $(\Delta T_{AD}^{max})_{T_2} = 12 \text{ K}$. However, undoubtedly important is the ability to realize in the material maximum values of both BCE at low pressure.

Estimates made using the following relation $p_{min} = T\Delta S / (C_{LAT}dT/dp)$, valid for phase transitions of the first order [9], show that the value $(\Delta S_{BCE}^{max})_{T_2}$ can be implemented in NH_4HSO_4 by rather insignificant pressure 0.1 GPa. In fact, the rather large value $(\Delta S_{BCE})_{T_2} = 0.95(\Delta S_{BCE}^{max})_{T_2}$ can be achieved even at much lower pressure, $p \approx 0.02 \text{ GPa}$ (Fig. 4(a)). However, intensive BCE, which also depends on the dS_{LAT}/dT derivative, is characterized by lower increase rate under pressure and reaches $(\Delta T_{AD}^{max})_{T_2}$ at about 0.13 GPa (Fig. 4(b)). As to the second order phase transition, at pressure 0.1 GPa extensive and intensive effects reach only about 18% of $(\Delta S_{BCE}^{max})_{T_1}$ and $(\Delta T_{AD}^{max})_{T_1}$.

At the second stage, effect of the lattice entropy change under pressure

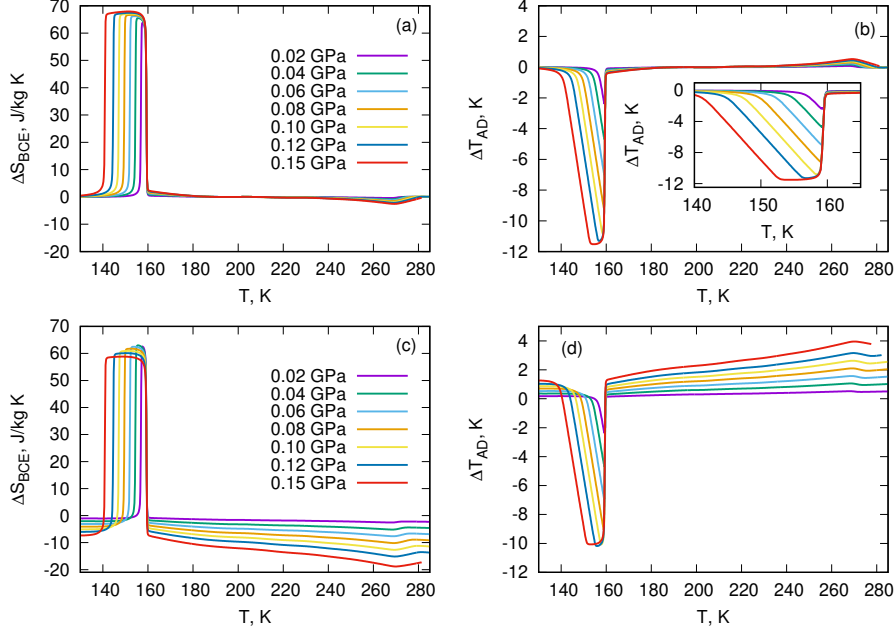


Figure 4: (a) Barocaloric entropy and (b) adiabatic temperature changes at different hydrostatic pressure in a wide temperature range determined without taking into account the effect of thermal expansion of the crystal lattice. Effect of thermal expansion of the crystal lattice on (c) ΔS_{BCE} and (d) ΔT_{AD}

on BCE in NH_4HSO_4 was studied. This contribution can be evaluated using Maxwell relation $(\partial S_{LAT}/\partial p)_T = -(\partial V/\partial T)_p$

$$\Delta S_{LAT}(T, p) = - \int_0^p (\partial V/\partial T)_p dp \approx -V_m \beta_{LAT}(T)p. \quad (2)$$

Here $V_m = 6.17 \times 10^{-5} \text{ m}^3/\text{mol}$ is the molar volume.

Taken into account the data of the thermal expansion study of the related $(\text{NH}_4)_2\text{SO}_4$ [15], it was suggested that the values of β_{LAT} and V_m of NH_4HSO_4 are also weakly depend on the pressure. Lattice contribution was determined
 135 from the results of dilatometric study of NH_4HSO_4 [19].

Fig. 4(c) and (d) demonstrate that due to the same sign of both derivatives, $(\partial V/\partial T)_{T1}$ and $(\partial V_{LAT}/\partial T)$, there is a strong increase in BCE_{conv} . At $p=0.15 \text{ GPa}$, the values $(\Delta S_{BCE})_{T1} = -18.8 \pm 1.5 \text{ J/kg}\cdot\text{K}$ and $(\Delta T_{AD})_{T1} = 4.0 \pm 0.2 \text{ K}$ are about one and a half times higher than even the maximum

140 values considered above as associated with the phase transition entropy ΔS_1 .
 Thus, contributions of $(\Delta S_{BCE}^{LAT})_{T_1}$ and $(\Delta T_{AD}^{LAT})_{T_1}$ to the full BCE at T_1 are
 predominant.

On the other hand, at the same pressure, BCE_{inv} associated with the phase
 transition $Pc-P1$ ($(\partial V/\partial T)_{T_2} < 0$), is reduced to the magnitudes $(\Delta S_{BCE})_{T_2} =$
 145 59 ± 5 J/kg·K, $(\Delta T_{AD})_{T_2} = -10.0 \pm 0.8$ K by BCE_{conv}^{LAT} arising in accordance
 with Eq. 2, $(\partial V_{LAT}/\partial T) > 0$: $(\Delta S_{BCE}^{LAT})_{T_2} = -9.0 \pm 0.7$ J/kg·K, $(\Delta T_{AD}^{LAT})_{T_2} =$
 1.5 ± 0.1 K.

At last, at the third stage, we determine the behavior of extensive and in-
 tensive BCE at T_2 taken into account the peculiarities of experiments with
 150 DTA under pressure. As it was discussed above, increase in pressure strongly
 decreases the entropy jump δS_2 at the first order phase transition $Pc - P1$
 (Fig. 2(b) and (d)), while the total entropy change ΔS_2 remains constant. Ana-
 lyzing the dependencies $S(T, p)$ using both the DTA data under pressure and the
 effect of the lattice expansion, barocaloric parameters at T_2 are determined and
 155 presented in Fig. 5 in comparison with the data obtained in the second stage.
 One can see that in this case the magnitudes of $(\Delta S_{BCE}^{max})_{T_2}$ and $(\Delta T_{AD}^{max})_{T_2}$ are
 realized at almost the same low pressure which was determined in the second
 stage (Fig. 4(c) and (d)). The main difference was observed in the form of peaks
 $(\Delta S_{BCE})_{T_2}(T)$ and $(\Delta T_{AD})_{T_2}(T)$ which is due to peculiarities of the processes
 160 of measuring the heat capacity by methods of adiabatic calorimeter and DTA.

Returning to the results of the BCE study at T_1 , one can confidently ar-
 gue that it would be interesting and useful to investigate the influence of the
 thermal expansion of the crystal lattice on conventional BCE in ferroelectrics
 characterized by large β_{LAT} and undergoing order–disorder transformation with
 165 the positive baric coefficient.

4. Conclusion

This paper demonstrates BCE in NH_4HSO_4 undergoing two successive ferro-
 electric phase transitions characterized by significantly different entropy changes

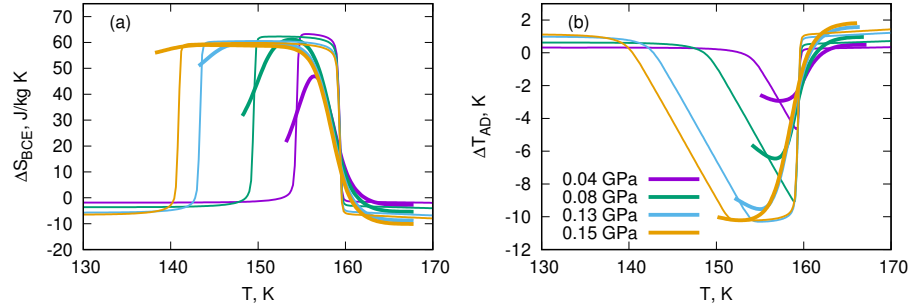


Figure 5: (a) Barocaloric entropy and (b) adiabatic temperature changes at different hydrostatic pressure determined using DTA data on a jump of the entropy (thick lines) and data presented in Fig. 4(c) and (d) (thin lines).

($\Delta S_1=1.2$ J/mol·K, $\Delta S_2=7.6$ J/mol·K) and large baric coefficients of different
 170 sign ($dT_1/dp=+90$ K/GPa and $dT_2/dp=-123$ K/GPa). Hydrostatic pressure
 strongly decreases the entropy jump at T_2 which reaches zero at a pressure of
 0.17 GPa. Very low pressure is needed to realize the maximum values of the
 extensive and intensive inverse BCE. Large thermal expansion of the crystal lat-
 tice leads to two very important points. Firstly, the conventional BCE can be
 175 greatly increased to values much higher than the magnitudes corresponding to
 the entropy of the phase transition. Secondly, in the case of the negative baric
 coefficient, a conversion from the inverse to conventional BCE can be realized
 by low pressure in the narrow temperature range.

References

- 180 [1] K. A. Gschneidner Jr, V. K. Pecharsky, A. O. Tsokol, Recent developments
 in magnetocaloric materials, Rep. Prog. Phys. 68 (6) (2005) 1479–1539.
 doi:10.1088/0034-4885/68/6/r04.
- [2] M. Valant, Electrocaloric materials for future solid-state refrigeration tech-
 nologies, Prog. Mater. Sci. 57 (6) (2012) 980 – 1009. doi:10.1016/j.
 185 pmatsci.2012.02.001.

- [3] X. Moya, S. Kar-Narayan, N. D. Mathur, Caloric materials near ferroic phase transitions, *Nat. Mater.* 13 (2014) 439–450. doi:10.1038/nmat3951.
- [4] H. Khassaf, T. Patel, R. J. Hebert, S. P. Alpay, Flexocaloric response of epitaxial ferroelectric films, *J. Appl. Phys.* 123 (2) (2018) 024102. doi:10.1063/1.5009121.
- 190
- [5] U. Tomc, J. Tušek, A. Kitanovski, A. Poredoš, A new magnetocaloric refrigeration principle with solid-state thermoelectric thermal diodes, *Appl. Thermal Engineering* 58 (1) (2013) 1–10. doi:10.1016/j.applthermaleng.2013.03.063.
- [6] U. Plaznik, M. Vrabelj, Z. Kutnjak, B. Malič, A. Poredoš, A. Kitanovski, Electrocaloric cooling: The importance of electric-energy recovery and heat regeneration, *EPL (Europhysics Letters)* 111 (5) (2015) 57009. doi:10.1209/0295-5075/111/57009.
- 195
- [7] A. Kitanovski, U. Plaznik, U. Tomc, A. Poredo, Present and future caloric refrigeration and heat-pump technologies, *Int. J. Refrigeration* 57 (2015) 288 – 298. doi:10.1016/j.ijrefrig.2015.06.008.
- 200
- [8] N. Michaelis, F. Welsch, S.-M. Kirsch, M. Schmidt, S. Seelecke, A. Schütze, Experimental parameter identification for elastocaloric air cooling, *Int. J. Refrigeration* 100 (2019) 167 – 174. doi:10.1016/j.ijrefrig.2019.01.006.
- 205
- [9] M. Gorev, E. Bogdanov, I. Flerov, T-p phase diagrams and the barocaloric effect in materials with successive phase transitions, *J. Phys. D: Appl. Phys.* 50 (38) (2017) 384002. doi:10.1088/1361-6463/aa8025.
- [10] M. Gorev, E. Bogdanov, I. Flerov, Conventional and inverse barocaloric effects around triple points in ferroelastics $(\text{NH}_4)_3\text{NbOF}_6$ and $(\text{NH}_4)_3\text{TiOF}_5$, *Scripta Materialia* 139 (2017) 53–57. doi:10.1016/j.scriptamat.2017.06.022.
- 210

- [11] E. Mikhaleva, I. Flerov, A. Kartashev, M. Gorev, A. Cherepakhin, K. Sablina, N. Mikhashenok, N. Volkov, A. Shabanov, Caloric effects and phase transitions in ferromagnetic-ferroelectric composites $x\text{La}_{0.7}\text{Pb}_{0.3}\text{MnO}_3-(1-x)\text{PbTiO}_3$, *J. Mater. Res.* 28 (24) (2013) 3322–3331. doi:10.1557/jmr.2013.360.
- [12] K. Alex Müller, F. Fauth, S. Fischer, M. Koch, A. Furrer, P. Lacorre, Cooling by adiabatic pressure application in $\text{Pr}_{1-x}\text{La}_x\text{NiO}_3$, *Appl. Phys. Letters* 73 (8) (1998) 1056–1058. doi:10.1063/1.122083.
- [13] T. Strässle, A. Furrer, Z. Hossain, C. Geibel, Magnetic cooling by the application of external pressure in rare-earth compounds, *Phys. Rev. B* 67 (2003) 054407. doi:10.1103/PhysRevB.67.054407.
- [14] N. A. de Oliveira, Barocaloric effect and the pressure induced solid state refrigerator, *J. Appl. Phys.* 109 (5) (2011) 053515. doi:10.1063/1.3556740.
- [15] P. Lloveras, E. Stern-Taulats, M. Barrio, J.-L. Tamarit, S. Crossley, W. Li, V. Pomjakushin, A. Planes, L. Manosa, N. D. Mathur, X. Moya, Giant barocaloric effects at low pressure in ferroelectric ammonium sulphate, *Nat. Commun.* 6 (2015) 8801. doi:10.1038/ncomms9801.
- [16] H. Khassaf, T. Patel, S. P. Alpay, Combined intrinsic elastocaloric and electrocaloric properties of ferroelectrics, *J. Appl. Phys.* 121 (14) (2017) 144102. doi:10.1063/1.4980098.
- [17] Y. Liu, J. Wei, P.-E. Janolin, I. C. Infante, X. Lou, B. Dkhil, Giant room-temperature barocaloric effect and pressure-mediated electrocaloric effect in BaTiO_3 single crystal, *Appl. Phys. Letters* 104 (16) (2014) 162904. doi:10.1063/1.4873162.
- [18] M. V. Gorev, I. N. Flerov, E. V. Bogdanov, V. N. Voronov, N. M. Laptash, Barocaloric effect near the structural phase transition in the $\text{Rb}_2\text{KTiOF}_5$ oxyfluoride, *Phys. Solid State* 52 (2) (2010) 377–383. doi:10.1134/S1063783410020253.

- [19] E. Mikhaleva, I. Flerov, A. Kartashev, M. Gorev, E. Bogdanov, V. Bondarev, Thermal, dielectric and barocaloric properties of NH_4HSO_4 crystallized from an aqueous solution and the melt, *Solid State Sciences* 67 (2017) 1–7. doi:10.1016/j.solidstatesciences.2017.03.004.
- 245 [20] R. Pepinsky, K. Vedam, S. Hoshino, Y. Okaya, Ammonium hydrogen sulfate: A new ferroelectric with low coercive field, *Phys. Rev.* 111 (1958) 1508–1510. doi:10.1103/PhysRev.111.1508.
- [21] D. Swain, V. S. Bhadram, P. Chowdhury, C. Narayana, Raman and x-ray investigations of ferroelectric phase transition in NH_4HSO_4 , *J. Phys. Chem. A* 116 (2012) 223–230. doi:10.1021/jp2075868.
- 250 [22] R. Pirc, Z. Kutnjak, R. Blinc, Q. M. Zhang, Upper bounds on the electrocaloric effect in polar solids, *Appl. Phys. Letters* 98 (2) (2011) 021909. doi:10.1063/1.3543628.

Conventional and inverse barocaloric effects in ferroelectric NH_4HSO_4

Mikhail V. Gorev^{a,b}, Ekaterina A. Mikhaleva^{a,b}, Igor N. Flerov^{a,b,*}, Evgeniy V. Bogdanov^{a,c}

^a*Kirensky Institute of Physics, Federal Research Center KSC SB RAS, Krasnoyarsk, Russia*

^b*Institute of Engineering Physics and Radioelectronics, Siberian Federal University, Krasnoyarsk, Russia*

^c*Institute of Engineering Systems and Energy, Krasnoyarsk State Agrarian University, 660049 Krasnoyarsk, Russia*

Abstract

In this study, the conventional and inverse barocaloric effects (BCE) in ferroelectric NH_4HSO_4 are reported. Maximum extensive and intensive BCE near order–disorder phase transition can be achieved at low pressure $p \leq 0.1$ GPa. Large thermal expansion of the crystal lattice plays a very important role in the developing conventional BCE and conversation between BCE of different sign in the narrow temperature range.

Keywords: Polymorphic phase transformation, Phase diagram, Order–disorder phenomena, Entropy, Barocaloric effect

PACS: 62.50.-p, 65.40.-b, 81.30.-t

1. Introduction

In recent years, much attention is paid to caloric effects (CE) in solids, particularly in ferroics, associated with the reversible change in the temperature, ΔT_{AD} , or entropy, ΔS_{CE} , under variation of the external field in adiabatic and isothermal conditions, respectively [1, 2, 3, 4]. One of the main reasons for this interest is related to the possibility to use the materials showing large CE's

*Corresponding author

Email addresses: gorev@iph.krasn.ru (Mikhail V. Gorev), katerina@iph.krasn.ru (Ekaterina A. Mikhaleva), flerov@iph.krasn.ru (Igor N. Flerov), evbogdanov@iph.krasn.ru (Evgeniy V. Bogdanov)

as solid state refrigerants in alternative cooling cycles [5, 6, 7, 8]. Among the CEs of different physical nature, the barocaloric effect (BCE) is distinguished by a serious advantage associated with its universality. Indeed, both extensive ΔS_{BCE} and intensive ΔT_{AD} barocaloric parameters strongly depend on the volume thermal expansion $(\partial V/\partial T)_p$ which very often shows large change near the temperature of any phase transitions: ferroelectric, ferroelastic, ferromagnetic

$$\Delta S_{BCE} = - \int_0^p \left(\frac{\partial V}{\partial T} \right)_p dp, \quad \Delta T_{AD} = - \frac{T}{C_p} \Delta S_{BCE}, \quad (1)$$

where C_p is the heat capacity.

The most intensively, BCE was studied in materials undergoing ferroelastic [9, 10] and ferromagnetic [11, 12, 13, 14] phase transitions. As to the ferro-
 5 electrics, their barocaloric efficiency was investigated only sporadically [11, 15, 16, 17]. It is known that the values and behavior of the BCE depend on the behavior and change in the entropy ΔS of the phase transition as well as on the sensitivity of the phase transition temperature to hydrostatic pressure [9, 10]. Thus, ferroics undergoing order–disorder transformations accompanied by large
 10 change in the volume and as result in baric coefficient, $dT_0/dp = \delta V/\delta S$, are the most promising barocaloric materials. Important requirements for caloric materials are also their low cost and ecological tolerance.

It has recently been shown that ferrielectric $(\text{NH}_4)_2\text{SO}_4$ meets all of the above requirements [15]. Due to significant values of $\Delta S=17 \text{ J/mol}\cdot\text{K} \approx R \ln 8$
 15 and $dT_0/dp=-45 \text{ K/GPa}$, rather large extensive and intensive BCE were observed in the region of the phase transition $Pnam - Pna2_1$ under low pressure. In accordance with Eq. 1, the negative baric coefficient associated with the negative value $(\partial V/\partial T)_p$ is the reason of the inverse BCE_{inv} in $(\text{NH}_4)_2\text{SO}_4$ accompanied by increase/decrease in entropy/temperature under pressure in-
 20 crease. It was also found that large coefficient of the volume thermal expansion of the crystal lattice, β_{LAT} , can play an important role in formation of real BCE in material. Indeed, in the case of ammonium sulphate, large positive value $\beta_{LAT} = 1.4 \times 10^{-4} \text{ K}^{-1}$ leads to decrease in the inverse BCE_{inv} under pressure due to the appearance of the conventional contribution BCE ($\Delta S_{BCE} < 0$,

$\Delta T_{AD} > 0$) [15]. The conversion from BCE_{inv} to BCE_{conv} was observed in a narrow temperature range. When pressure increases, the ratio between these values changes and at $p=0.25$ GPa is about $BCE_{conv}/BCE_{inv}=0.15$. Thus, to get correct information on BCE in materials with large thermal expansion coefficient, it is necessary to take into account the effect of pressure on the lattice entropy. It is obvious that the magnitude of baric coefficient strongly effects on the maximum value of the intensive BCE [18]. In this respect, it is interesting to analyze both BCE in material with anomalously large negative or positive dT/dp . From this point of view, another ferroelectric crystal, ammonium hydrogen sulphate, is very good example.

Indeed, NH_4HSO_4 undergoes two successive phase transitions $P2_1/c \leftrightarrow Pc \leftrightarrow P1$, of the strong second and first order at $T_1=271$ K and $T_2=159$ K, respectively. One more difference is that anomaly of volumetric thermal expansion coefficient is positive at T_1 and negative at T_2 [19] which leads to BCE_{conv} and BCE_{inv} . Thus, the contribution from the thermal expansion of the crystal lattice to both BCE will be also different. Despite the large difference in the entropy of the phase transitions ($\Delta S_1=1.2$ J/mol·K, $\Delta S_2=7.6$ J/mol·K), one can suppose that BCE_{conv} at T_1 could be strongly increased due to rather large value of $\beta_{LAT}=2 \times 10^{-4}$ K $^{-1}$ far from the phase transition points. In addition, like $(NH_4)_2SO_4$, ammonium hydrogen sulphate is also easy to prepare, cheap and environmentally friendly.

In the present paper, we performed an analysis of extensive and intensive barocaloric efficiency of NH_4HSO_4 near both phase transformations based on methods developed by us earlier [18]. For this aim, the dependencies of $\Delta T_{AD}(T, p)$ and $\Delta S_{BCE}(T, p)$ were determined using data on total and anomalous heat capacity [19], the $T-p$ phase diagram and the dependencies of entropy of the phase transitions on temperature and pressure.

2. Experimental details

Powder samples of ammonium hydrogen sulphate were obtained by slow evaporation at 45°C from an aqueous solution containing equimolar quantities
55 of high purity raw materials $(\text{NH}_4)_2\text{SO}_4$ and H_2SO_4 .

The quality of samples used for the experiments was checked at room temperature using XRD, which revealed a monoclinic symmetry consistent with the space group $P2_1/c$ ($Z=8$) suggested in Refs. [20, 21]. No additional phases were observed in the samples. Fig. 1 shows the results of Rietveld refinement.
60 The unit cell parameters $a = 24.770(6)\text{\AA}$, $b = 4.611(1)\text{\AA}$, $c = 14.871(4)\text{\AA}$, $\beta = 89.70(1)$ grad are consistent with the values determined in Ref. [21].

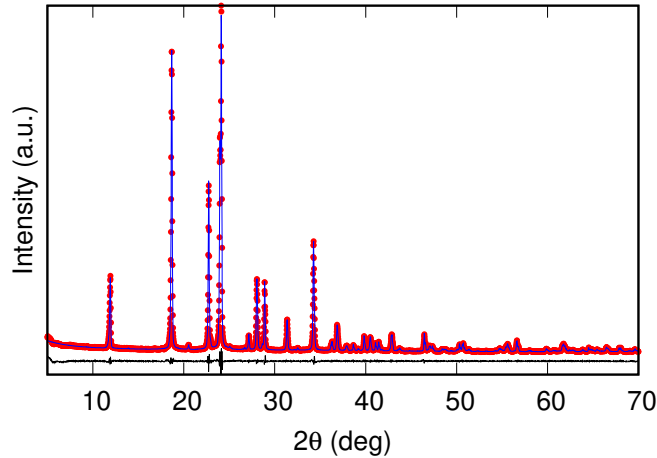


Figure 1: Difference Rietveld plot for NH_4HSO_4 at room temperature.

Quasi-ceramic samples of NH_4HSO_4 in the form of disks, approximately 1.0 mm thick and approximately 6 mm in diameter, were used for investigations. Because of the presence of ammonium ion in crystal, the heat treatments of
65 ceramics were not performed. For dielectric measurements, electrodes on pellets were formed by conducting glue covered the opposite sides of the sample.

The effect of hydrostatic pressure on temperature and entropy of the phase transitions was studied using a piston-cylinder type vessel associated with a pressure multiplier. Pressure of up to 0.25 GPa was generated using a mixture

70 of silicon oil and pentane exhibiting optimal electrical and heat conductivity, solidification point and viscosity as the pressure-transmitting medium. Pressure and temperature were measured using a manganin resistive sensor and a copper-constantan thermocouple, with accuracies of about $\pm 10^{-3}$ GPa and ± 0.3 K respectively.

75 The dependencies $T_1(p)$ and $T_2(p)$ were revealed, firstly, in experiments with differential thermal analysis (DTA) and, secondly, by measurements of the permittivity ε . In the former case, to detect anomalies of DTA-signal associated with the heat capacity anomalies, high-sensitive differential copper-germanium thermocouple was used. In the latter case, experiments were performed using
80 an E7-20 immittance meter. To ensure the reliability of the results, the measurements were performed for both increasing and decreasing pressure cycles.

3. Results and discussion

At ambient pressure, the anomalies of DTA signal and ε were detected at about $T_1 = 271.5 \pm 1.0$ K and $T_2 = 160 \pm 2$ K (Fig. 2 (a) and (b)), which agree well
85 with values observed during measurements of the heat capacity [19]. Fig. 2(c) shows that an increase in pressure leads to linear increase and decrease in T_1 and T_2 , respectively: $dT_1/dp = +90 \pm 15$ K/GPa and $dT_2/dp = -123 \pm 15$ K/GPa which are significantly higher than that for ammonium sulfate [15].

Due to the limited sensitivity of the DTA method, the area under the DTA
90 peak at T_2 represents a change in the enthalpy δH_2 (entropy $\delta S_2 = \delta H_2/T_2$) jump at the first order phase transition $Pc \leftrightarrow P1$ in NH_4HSO_4 . An increase in pressure is accompanied by a linear decrease in the value of δS_2 which reaches zero at $p \approx 0.17$ GPa (Fig. 2(d)) that can be considered as corresponding to the pressure of the tricritical point. On the other hand, it is unlikely that such a low
95 pressure may affect the degree of disordering of structural elements in phases $P2_1/c$ and Pc , and as a result the total entropy change at the $Pc \leftrightarrow P1$ transformation, $\Delta S_2(p) = \delta S_2(p) + \Delta S_2^*(T, p)$, remains constant. Here $\Delta S_2^*(T, p)$ is the temperature- and pressure-dependent contribution.

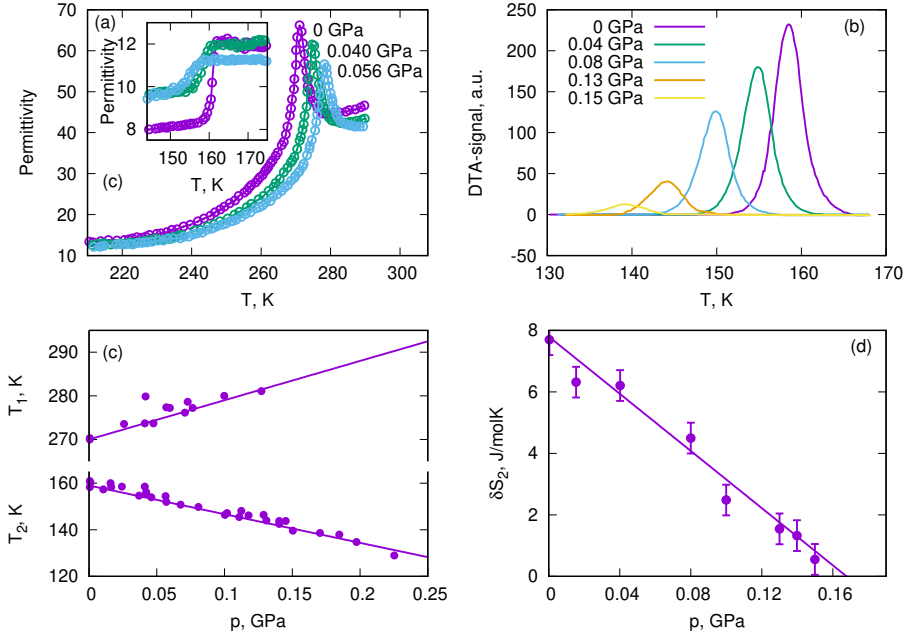


Figure 2: (a) Temperature dependencies of permittivity for NH_4HSO_4 around T_1 and T_2 and (b) anomalous component of the DTA signal near T_2 at different hydrostatic pressure. (c) Temperature – pressure phase diagram combining the results on the DTA signal and permittivity study. (d) Entropy jump δS_2 for the first-order transition in NH_4HSO_4 at different hydrostatic pressure.

The analysis of extensive and intensive BCE in NH_4HSO_4 was performed in three steps.

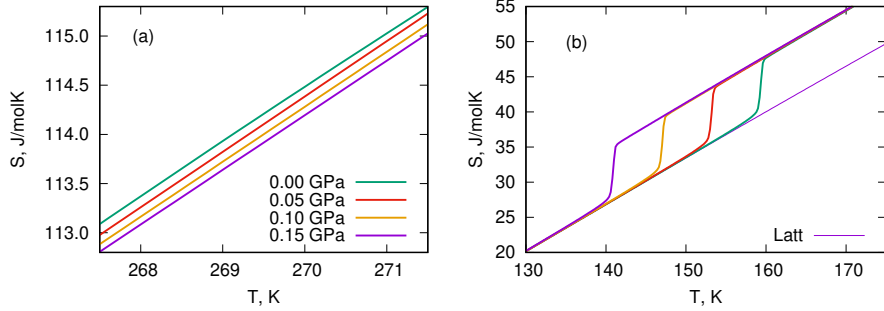


Figure 3: Temperature dependencies of total entropy of NH_4HSO_4 at different hydrostatic pressure near (a) T_1 and (b) T_2 .

At the first stage, the possible influence of pressure on the entropy of the crystal lattice ΔS_{LAT} was not taken into account. Fig. 3 demonstrates the temperature behavior of the lattice $S_{LAT}(T) - S_{LAT}(100 \text{ K}) = \int_{100}^T (C_{LAT}/T) dT$ and total $S = \int_{100}^T (C_p/T) dT$ entropies in the vicinities of T_1 and T_2 . Temperature dependencies $S(T)$ under pressure were determined by summation of the lattice entropy S_{LAT} and the anomalous contributions ΔS_1 and ΔS_2 shifted along the temperature scale in accordance with the sign of baric coefficients dT_1/dp and dT_2/dp . The values and behavior of extensive BCE, ΔS_{BCE} , at different pressure were determined from temperature dependencies of the total entropy as a difference $\Delta S_{BCE} = S(T, p) - S(T, p = 0)$ at constant temperature (Fig. 4(a)). The temperature dependencies of the intensive BCE were revealed analyzing plots of $S(T, p) = S_{LAT}(T, p = 0) + \Delta S(T, p)$ at constant entropy $S(T, p) = S(T + \Delta T_{AD}, p = 0)$ (Fig. 4(b)). Large difference in BCE at T_1 and T_2 at the same pressure is the result of the different values of ΔS_1 and ΔS_2 .

It is known [22] that if we neglect the contribution of the thermal expansion of the crystal lattice, the maximum values of both BCE are limited by the value of the entropy of the phase transition: $(\Delta S_{BCE}^{max})_{T_1} = \Delta S_1 = -10 \text{ J/kg}\cdot\text{K}$, $(\Delta T_{AD}^{max})_{T_1} = 2 \text{ K}$; $(\Delta S_{BCE}^{max})_{T_2} = \Delta S_2 = 68 \text{ J/kg}\cdot\text{K}$, $(\Delta T_{AD}^{max})_{T_2} = 12 \text{ K}$. However, undoubtedly important is the ability to realize in the material maximum values of both BCE at low pressure.

Estimates made using the following relation $p_{min} = T\Delta S/(C_{LAT}dT/dp)$, valid for phase transitions of the first order [9], show that the value $(\Delta S_{BCE}^{max})_{T_2}$ can be implemented in NH_4HSO_4 by rather insignificant pressure 0.1 GPa. In fact, the rather large value $(\Delta S_{BCE})_{T_2} = 0.95(\Delta S_{BCE}^{max})_{T_2}$ can be achieved even at much lower pressure, $p \approx 0.02 \text{ GPa}$ (Fig. 4(a)). However, intensive BCE, which also depends on the dS_{LAT}/dT derivative, is characterized by lower increase rate under pressure and reaches $(\Delta T_{AD}^{max})_{T_2}$ at about 0.13 GPa (Fig. 4(b)). As to the second order phase transition, at pressure 0.1 GPa extensive and intensive effects reach only about 18% of $(\Delta S_{BCE}^{max})_{T_1}$ and $(\Delta T_{AD}^{max})_{T_1}$.

At the second stage, effect of the lattice entropy change under pressure on BCE in NH_4HSO_4 was studied. This contribution can be evaluated using

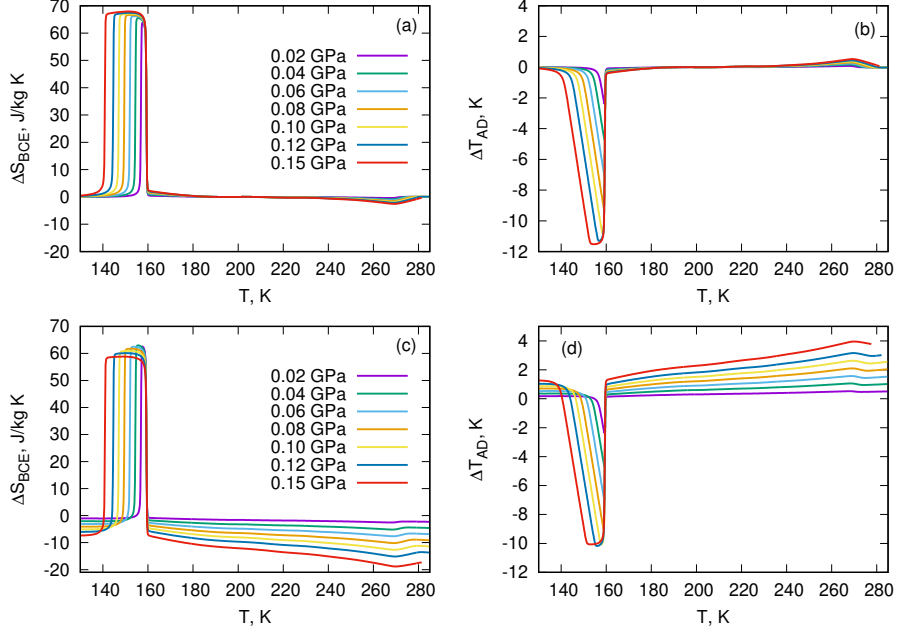


Figure 4: (a) Barocaloric entropy and (b) adiabatic temperature changes at different hydrostatic pressure in a wide temperature range determined without taking into account the effect of thermal expansion of the crystal lattice. Effect of thermal expansion of the crystal lattice on (c) ΔS_{BCE} (d) ΔT_{AD}

Maxwell relation $(\partial S_{LAT}/\partial p)_T = -(\partial V/\partial T)_p$

$$\Delta S_{LAT}(T, p) = - \int_0^p (\partial V/\partial T)_p dp \approx -V_m \beta_{LAT}(T)p. \quad (2)$$

130 Here $V_m = 6.17 \times 10^{-5} \text{ m}^3/\text{mol}$ is the molar volume.

Taken into account the data of the thermal expansion study of the related $(\text{NH}_4)_2\text{SO}_4$ [15], it was suggested that the values of β_{LAT} and V_m of NH_4HSO_4 are also weakly depend on the pressure. Lattice contribution was determined from the results of dilatometric study of NH_4HSO_4 [19].

135 Fig. 4(c) and (d) demonstrate that due to the same sign of both derivatives, $(\partial V/\partial T)_{T1}$ and $(\partial V_{LAT}/\partial T)$, there is a strong increase in BCE_{conv} . At $p=0.15 \text{ GPa}$, the values $(\Delta S_{BCE})_{T1} = -18.8 \pm 1.5 \text{ J/kg}\cdot\text{K}$ and $(\Delta T_{AD})_{T1} = 4.0 \pm 0.2 \text{ K}$ are about one and a half times higher than even the maximum values considered above as associated with the phase transition entropy ΔS_1 .

140 Thus, contributions of $(\Delta S_{BCE}^{LAT})_{T_1}$ and $(\Delta T_{AD}^{LAT})_{T_1}$ to the full BCE at T_1 are predominant.

On the other hand, at the same pressure, BCE_{inv} associated with the phase transition $Pc-P1$ ($(\partial V/\partial T)_{T_2} < 0$), is reduced to the magnitudes $(\Delta S_{BCE})_{T_2} = 59 \pm 5$ J/kg·K, $(\Delta T_{AD})_{T_2} = -10.0 \pm 0.8$ K by BCE_{conv}^{LAT} arising in accordance
 145 with Eq. 2, $(\partial V_{LAT}/\partial T) > 0$: $(\Delta S_{BCE}^{LAT})_{T_2} = -9.0 \pm 0.7$ J/kg·K, $(\Delta T_{AD}^{LAT})_{T_2} = 1.5 \pm 0.1$ K.

At last, at the third stage, we determine the behavior of extensive and intensive BCE at T_2 taken into account the peculiarities of experiments with DTA under pressure. As it was discussed above, increase in pressure strongly
 150 decreases the entropy jump δS_2 at the first order phase transition $Pc - P1$ (Fig. 2(b) and (d)), while the total entropy change ΔS_2 remains constant. Analyzing the dependencies $S(T, p)$ using both the DTA data under pressure and the effect of the lattice expansion, barocaloric parameters at T_2 are determined and presented in Fig. 5 in comparison with the data obtained in the second stage.
 155 One can see that in this case the magnitudes of $(\Delta S_{BCE}^{max})_{T_2}$ and $(\Delta T_{AD}^{max})_{T_2}$ are realized at almost the same low pressure which was determined in the second stage (Fig. 4(c) and (d)). The main difference was observed in the form of peaks $(\Delta S_{BCE})_{T_2}(T)$ and $(\Delta T_{AD})_{T_2}(T)$ which is due to peculiarities of the processes of measuring the heat capacity by methods of adiabatic calorimeter and DTA.

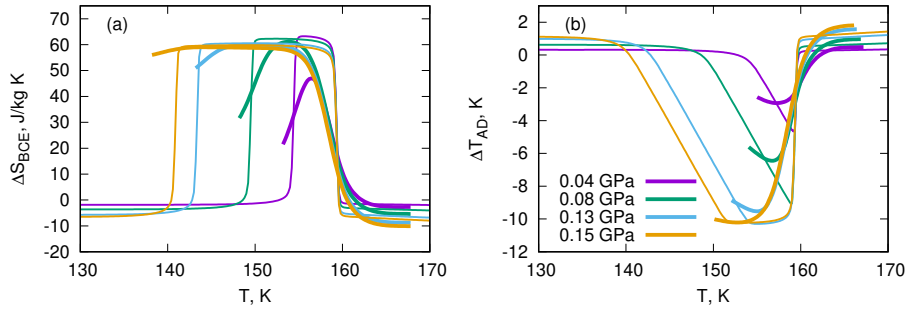


Figure 5: (a) Barocaloric entropy and (b) adiabatic temperature changes at different hydrostatic pressure determined using DTA data on a jump of the entropy (thick lines) and data presented in Fig. 4(c) and (d) (thin lines).

160 Returning to the results of the BCE study at T_1 , one can confidently argue that it would be interesting and useful to investigate the influence of the thermal expansion of the crystal lattice on conventional BCE in ferroelectrics characterized by large β_{LAT} and undergoing order–disorder transformation with the positive baric coefficient.

165 4. Conclusion

This paper demonstrates BCE in NH_4HSO_4 undergoing two successive ferroelectric phase transitions of displacive and order–disorder type at T_1 and at T_2 , respectively. Both transformations are characterized by large baric coefficients of different sign. Hydrostatic pressure strongly decreases the entropy jump at T_2 which reaches zero at a pressure of 0.17 GPa. Very low pressure is needed to realize the maximum values of the extensive and intensive inverse BCE. Large thermal expansion of the crystal lattice leads to two very important points. Firstly, the conventional BCE can be greatly increased to values much higher than the magnitudes corresponding to the entropy of the phase transition. Secondly, in the case of the negative baric coefficient, a conversion from the inverse to conventional BCE can be realized by low pressure in the narrow temperature range.

References

- [1] K. A. Gschneidner Jr, V. K. Pecharsky, A. O. Tsokol, Recent developments in magnetocaloric materials, Rep. Prog. Phys. 68 (6) (2005) 1479–1539. doi:10.1088/0034-4885/68/6/r04.
- [2] M. Valant, Electrocaloric materials for future solid-state refrigeration technologies, Prog. Mater. Sci. 57 (6) (2012) 980 – 1009. doi:10.1016/j.pmatsci.2012.02.001.
- [3] X. Moya, S. Kar-Narayan, N. D. Mathur, Caloric materials near ferroic phase transitions, Nat. Mater. 13 (2014) 439–450. doi:10.1038/nmat3951.

- [4] H. Khassaf, T. Patel, R. J. Hebert, S. P. Alpay, Flexocaloric response of epitaxial ferroelectric films, *J. Appl. Phys.* 123 (2) (2018) 024102. doi:10.1063/1.5009121.
- 190 [5] U. Tomc, J. Tušek, A. Kitanovski, A. Poredoš, A new magnetocaloric refrigeration principle with solid-state thermoelectric thermal diodes, *Appl. Thermal Engineering* 58 (1) (2013) 1–10. doi:10.1016/j.applthermaleng.2013.03.063.
- [6] U. Plaznik, M. Vrabelj, Z. Kutnjak, B. Malič, A. Poredoš, A. Kitanovski, 195 Electrocaloric cooling: The importance of electric-energy recovery and heat regeneration, *EPL (Europhysics Letters)* 111 (5) (2015) 57009. doi:10.1209/0295-5075/111/57009.
- [7] A. Kitanovski, U. Plaznik, U. Tomc, A. Poredo, Present and future caloric refrigeration and heat-pump technologies, *Int. J. Refrigeration* 57 (2015) 200 288 – 298. doi:10.1016/j.ijrefrig.2015.06.008.
- [8] N. Michaelis, F. Welsch, S.-M. Kirsch, M. Schmidt, S. Seelecke, A. Schütze, Experimental parameter identification for elastocaloric air cooling, *Int. J. Refrigeration* 100 (2019) 167 – 174. doi:10.1016/j.ijrefrig.2019.01.006.
- 205 [9] M. Gorev, E. Bogdanov, I. Flerov, T-p phase diagrams and the barocaloric effect in materials with successive phase transitions, *J. Phys. D: Appl. Phys.* 50 (38) (2017) 384002. doi:10.1088/1361-6463/aa8025.
- [10] M. Gorev, E. Bogdanov, I. Flerov, Conventional and inverse barocaloric effects around triple points in ferroelastics $(\text{NH}_4)_3\text{NbOF}_6$ and $(\text{NH}_4)_3\text{TiOF}_5$, 210 *Scripta Materialia* 139 (2017) 53–57. doi:10.1016/j.scriptamat.2017.06.022.
- [11] E. Mikhaleva, I. Flerov, A. Kartashev, M. Gorev, A. Cherepakhin, K. Sablina, N. Mikhashenok, N. Volkov, A. Shabanov, Caloric effects and phase transitions in ferromagnetic-ferroelectric composites $x\text{La}_{0.7}\text{Pb}_0$.

- 215 $_3\text{MnO}_3\text{-(1-x)PbTiO}_3$, *J. Mater. Res.* 28 (24) (2013) 3322–3331. doi: 10.1557/jmr.2013.360.
- [12] K. Alex Müller, F. Fauth, S. Fischer, M. Koch, A. Furrer, P. Lacorre, Cooling by adiabatic pressure application in $\text{Pr}_{1-x}\text{La}_x\text{NiO}_3$, *Appl. Phys. Letters* 73 (8) (1998) 1056–1058. doi:10.1063/1.122083.
- 220 [13] T. Strässle, A. Furrer, Z. Hossain, C. Geibel, Magnetic cooling by the application of external pressure in rare-earth compounds, *Phys. Rev. B* 67 (2003) 054407. doi:10.1103/PhysRevB.67.054407.
- [14] N. A. de Oliveira, Barocaloric effect and the pressure induced solid state refrigerator, *J. Appl. Phys.* 109 (5) (2011) 053515. doi:10.1063/1.3556740.
- 225 [15] P. Lloveras, E. Stern-Taulats, M. Barrio, J.-L. Tamarit, S. Crossley, W. Li, V. Pomjakushin, A. Planes, L. Manosa, N. D. Mathur, X. Moya, Giant barocaloric effects at low pressure in ferroelectric ammonium sulphate, *Nat. Commun.* 6 (2015) 8801. doi:10.1038/ncomms9801.
- [16] H. Khassaf, T. Patel, S. P. Alpay, Combined intrinsic elastocaloric and electrocaloric properties of ferroelectrics, *J. Appl. Phys.* 121 (14) (2017) 144102. doi:10.1063/1.4980098.
- 230 [17] Y. Liu, J. Wei, P.-E. Janolin, I. C. Infante, X. Lou, B. Dkhil, Giant room-temperature barocaloric effect and pressure-mediated electrocaloric effect in BaTiO_3 single crystal, *Appl. Phys. Letters* 104 (16) (2014) 162904. doi: 10.1063/1.4873162.
- 235 [18] M. V. Gorev, I. N. Flerov, E. V. Bogdanov, V. N. Voronov, N. M. Laptash, Barocaloric effect near the structural phase transition in the $\text{Rb}_2\text{KTiOF}_5$ oxyfluoride, *Phys. Solid State* 52 (2) (2010) 377–383. doi: 10.1134/S1063783410020253.
- 240 [19] E. Mikhaleva, I. Flerov, A. Kartashev, M. Gorev, E. Bogdanov, V. Bondarev, Thermal, dielectric and barocaloric properties of NH_4HSO_4 crystal-

lized from an aqueous solution and the melt, *Solid State Sciences* 67 (2017) 1–7. doi:10.1016/j.solidstatesciences.2017.03.004.

- [20] R. Pepinsky, K. Vedam, S. Hoshino, Y. Okaya, Ammonium hydrogen sulfate: A new ferroelectric with low coercive field, *Phys. Rev.* 111 (1958) 1508–1510. doi:10.1103/PhysRev.111.1508.
- [21] D. Swain, V. S. Bhadram, P. Chowdhury, C. Narayana, Raman and x-ray investigations of ferroelectric phase transition in NH_4HSO_4 , *J. Phys. Chem. A* 116 (2012) 223–230. doi:10.1021/jp2075868.
- [22] R. Pirc, Z. Kutnjak, R. Blinc, Q. M. Zhang, Upper bounds on the electrocaloric effect in polar solids, *Appl. Phys. Letters* 98 (2) (2011) 021909. doi:10.1063/1.3543628.

Conventional and inverse barocaloric effects in ferroelectric NH_4HSO_4

Mikhail V. Gorev^{a,b}, Ekaterina A. Mikhaleva^{a,b}, Igor N. Flerov^{a,b,*}, Evgeniy V. Bogdanov^{a,c}

^a*Kirensky Institute of Physics, Federal Research Center KSC SB RAS, Krasnoyarsk, Russia*

^b*Institute of Engineering Physics and Radioelectronics, Siberian Federal University, Krasnoyarsk, Russia*

^c*Institute of Engineering Systems and Energy, Krasnoyarsk State Agrarian University, 660049 Krasnoyarsk, Russia*

Abstract

In this study, the conventional and inverse barocaloric effects (BCE) in ferroelectric NH_4HSO_4 are reported. Maximum extensive and intensive BCE near order–disorder phase transition can be achieved at low pressure $p \leq 0.1$ GPa. Large thermal expansion of the crystal lattice plays a very important role in the developing conventional BCE and conversation between BCE of different sign in the narrow temperature range.

Keywords: Polymorphic phase transformation, Phase diagram, Order–disorder phenomena, Entropy, Barocaloric effect

PACS: 62.50.-p, 65.40.-b, 81.30.-t

1. Introduction

In recent years, much attention is paid to caloric effects (CE) in solids, particularly in ferroics, associated with the reversible change in the temperature, ΔT_{AD} , or entropy, ΔS_{CE} , under variation of the external field in adiabatic and isothermal conditions, respectively [1, 2, 3, 4]. One of the main reasons for this interest is related to the possibility to use the materials showing large CE's

*Corresponding author

Email addresses: gorev@iph.krasn.ru (Mikhail V. Gorev), katerina@iph.krasn.ru (Ekaterina A. Mikhaleva), flerov@iph.krasn.ru (Igor N. Flerov), evbogdanov@iph.krasn.ru (Evgeniy V. Bogdanov)

as solid state refrigerants in alternative cooling cycles [5, 6, 7, 8]. Among the CE's of different physical nature, the barocaloric effect (BCE) is distinguished by a serious advantage associated with its universality. Indeed, both extensive ΔS_{BCE} and intensive ΔT_{AD} barocaloric parameters strongly depend on the volume thermal expansion $(\partial V/\partial T)_p$ which very often shows large change near the temperature of any phase transitions: ferroelectric, ferroelastic, ferromagnetic

$$\Delta S_{BCE} = - \int_0^p \left(\frac{\partial V}{\partial T} \right)_p dp, \quad \Delta T_{AD} = - \frac{T}{C_p} \Delta S_{BCE}, \quad (1)$$

where C_p is the heat capacity.

The most intensively, BCE was studied in materials undergoing ferroelastic [9, 10] and ferromagnetic [11, 12, 13, 14] phase transitions. As to the ferro-
 5 electrics, their barocaloric efficiency was investigated only sporadically [11, 15, 16, 17]. It is known that the values and behavior of the BCE depend on the behavior and change in the entropy ΔS of the phase transition as well as on the sensitivity of the phase transition temperature to hydrostatic pressure [9, 10]. Thus, ferroics undergoing order–disorder transformations accompanied by large
 10 change in the volume and as result in baric coefficient, $dT_0/dp = \delta V/\delta S$, are the most promising barocaloric materials. Important requirements for caloric materials are also their low cost and ecological tolerance.

It has recently been shown that ferrielectric $(\text{NH}_4)_2\text{SO}_4$ meets all of the above requirements [15]. Due to significant values of $\Delta S=17 \text{ J/mol}\cdot\text{K} \approx R \ln 8$
 15 and $dT_0/dp=-45 \text{ K/GPa}$, rather large extensive and intensive BCE were observed in the region of the phase transition $Pnam - Pna2_1$ under low pressure. In accordance with Eq. 1, the negative baric coefficient associated with the negative value $(\partial V/\partial T)_p$ is the reason of the inverse BCE_{inv} in $(\text{NH}_4)_2\text{SO}_4$ accompanied by increase/decrease in entropy/temperature under pressure in-
 20 crease. It was also found that large coefficient of the volume thermal expansion of the crystal lattice, β_{LAT} , can play an important role in formation of real BCE in material. Indeed, in the case of ammonium sulphate, large positive value $\beta_{LAT} = 1.4 \times 10^{-4} \text{ K}^{-1}$ leads to decrease in the inverse BCE_{inv} under pressure due to the appearance of the conventional contribution BCE ($\Delta S_{BCE} < 0$,

$\Delta T_{AD} > 0$) [15]. The conversion from BCE_{inv} to BCE_{conv} was observed in a narrow temperature range. When pressure increases, the ratio between these values changes and at $p=0.25$ GPa is about $BCE_{conv}/BCE_{inv}=0.15$. Thus, to get correct information on BCE in materials with large thermal expansion coefficient, it is necessary to take into account the effect of pressure on the lattice entropy. It is obvious that the magnitude of baric coefficient strongly effects on the maximum value of the intensive BCE [18]. In this respect, it is interesting to analyze both BCE in material with anomalously large negative or positive dT/dp . From this point of view, another ferroelectric crystal, ammonium hydrogen sulphate, is very good example.

Indeed, NH_4HSO_4 undergoes two successive phase transitions $P2_1/c \leftrightarrow Pc \leftrightarrow P1$, of the strong second and first order at $T_1=271$ K and $T_2=159$ K, respectively. One more difference is that anomaly of volumetric thermal expansion coefficient is positive at T_1 and negative at T_2 [19] which leads to BCE_{conv} and BCE_{inv} . Thus, the contribution from the thermal expansion of the crystal lattice to both BCE will be also different. Despite the large difference in the entropy of the phase transitions ($\Delta S_1=1.2$ J/mol·K, $\Delta S_2=7.6$ J/mol·K), one can suppose that BCE_{conv} at T_1 could be strongly increased due to rather large value of $\beta_{LAT}=2 \times 10^{-4}$ K $^{-1}$ far from the phase transition points. In addition, like $(NH_4)_2SO_4$, ammonium hydrogen sulphate is also easy to prepare, cheap and environmentally friendly.

In the present paper, we performed an analysis of extensive and intensive barocaloric efficiency of NH_4HSO_4 near both phase transformations based on methods developed by us earlier [18]. For this aim, the dependencies of $\Delta T_{AD}(T, p)$ and $\Delta S_{BCE}(T, p)$ were determined using data on total and anomalous heat capacity [19], the $T-p$ phase diagram and the dependencies of entropy of the phase transitions on temperature and pressure.

2. Experimental details

Powder samples of ammonium hydrogen sulphate were obtained by slow evaporation at 45°C from an aqueous solution containing equimolar quantities
55 of high purity raw materials $(\text{NH}_4)_2\text{SO}_4$ and H_2SO_4 .

The quality of samples used for the experiments was checked at room temperature using XRD, which revealed a monoclinic symmetry consistent with the space group $P2_1/c$ ($Z=8$) suggested in Refs. [20, 21]. No additional phases were observed in the samples. Fig. 1 shows the results of Rietveld refinement
60 ($R_{wp}=6.04$, $R_p=4.23$, $\chi^2=2.06$). The unit cell parameters $a = 24.770(6)\text{\AA}$, $b = 4.611(1)\text{\AA}$, $c = 14.871(4)\text{\AA}$, $\beta = 89.70(1)$ grad are consistent with the values determined in Ref. [21].

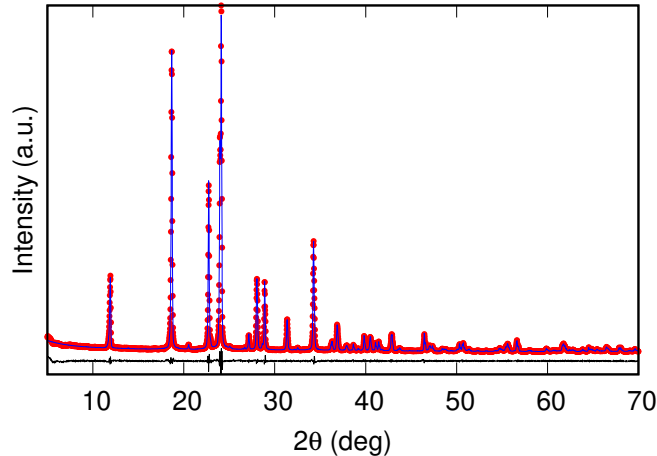


Figure 1: Difference Rietveld plot for NH_4HSO_4 at room temperature.

Quasi-ceramic samples of NH_4HSO_4 in the form of disks, approximately 1.0 mm thick and approximately 6 mm in diameter, were used for investigations.
65 Because of the presence of ammonium ion in crystal, the heat treatments of ceramics were not performed. For dielectric measurements, electrodes on pellets were formed by conducting glue covered the opposite sides of the sample.

The effect of hydrostatic pressure on temperature and entropy of the phase transitions was studied using a piston-cylinder type vessel associated with a

70 pressure multiplier. Pressure of up to 0.25 GPa was generated using a mixture
of silicon oil and pentane exhibiting optimal electrical and heat conductivity,
solidification point and viscosity as the pressure-transmitting medium. Pressure
and temperature were measured using a manganin resistive sensor and a copper-
constantan thermocouple, with accuracies of about $\pm 10^{-3}$ GPa and ± 0.3 K
75 respectively.

The dependencies $T_1(p)$ and $T_2(p)$ were revealed, firstly, in experiments with
differential thermal analysis (DTA) and, secondly, by measurements of the per-
mittivity ε . In the former case, to detect anomalies of DTA-signal associated
with the heat capacity anomalies, high-sensitive differential copper-germanium
80 thermocouple was used. In the latter case, experiments were performed using
an E7-20 immittance meter. To ensure the reliability of the results, the mea-
surements were performed for both increasing and decreasing pressure cycles.

3. Results and discussion

At ambient pressure, the anomalies of DTA signal and ε were detected at
85 about $T_1 = 271.5 \pm 1.0$ K and $T_2 = 160 \pm 2$ K (Fig. 2 (a) and (b)), which agree well
with values observed during measurements of the heat capacity [19]. Fig. 2(c)
shows that an increase in pressure leads to linear increase and decrease in T_1 and
 T_2 , respectively: $dT_1/dp = +90 \pm 15$ K/GPa and $dT_2/dp = -123 \pm 15$ K/GPa
which are significantly higher than that for ammonium sulfate [15].

90 Due to the limited sensitivity of the DTA method, the area under the DTA
peak at T_2 represents a change in the enthalpy δH_2 (entropy $\delta S_2 = \delta H_2/T_2$)
jump at the first order phase transition $Pc \leftrightarrow P1$ in NH_4HSO_4 . An increase in
pressure is accompanied by a linear decrease in the value of δS_2 which reaches
zero at $p \approx 0.17$ GPa (Fig. 2(d)) that can be considered as corresponding to the
95 pressure of the tricritical point. On the other hand, it is unlikely that such a low
pressure may affect the degree of disordering of structural elements in phases
 $P2_1/c$ and Pc , and as a result the total entropy change at the $Pc \leftrightarrow P1$ trans-
formation, $\Delta S_2(p) = \delta S_2(p) + \Delta S_2^*(T, p)$, remains constant. Here $\Delta S_2^*(T, p)$ is

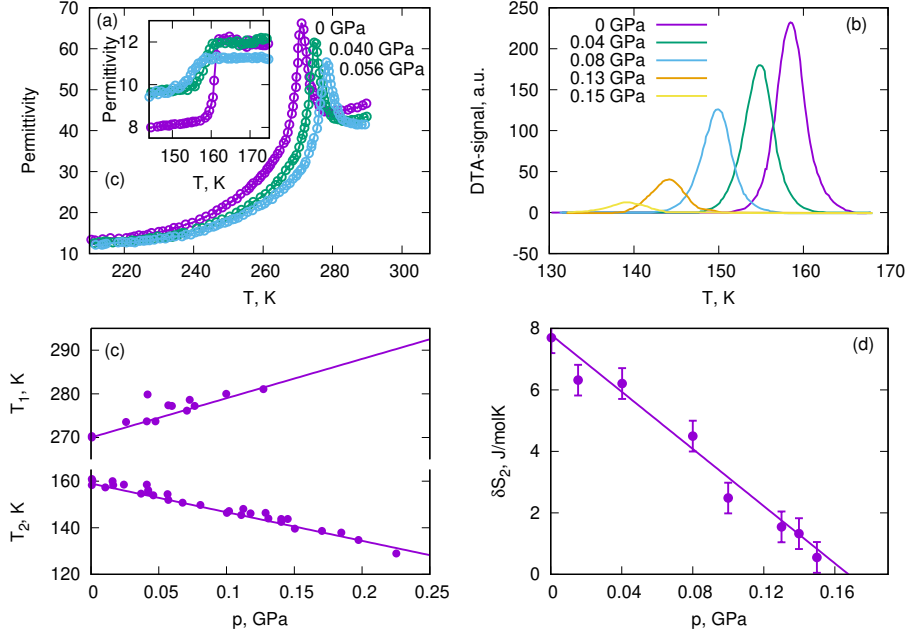


Figure 2: (a) Temperature dependencies of permittivity for NH_4HSO_4 around T_1 and T_2 and (b) anomalous component of the DTA signal near T_2 at different hydrostatic pressure. (c) Temperature – pressure phase diagram combining the results on the DTA signal and permittivity study. (d) Entropy jump δS_2 for the first-order transition in NH_4HSO_4 at different hydrostatic pressure.

the temperature- and pressure-dependent contribution.

100 The analysis of extensive and intensive BCE in NH_4HSO_4 was performed in three steps.

At the first stage, the possible influence of pressure on the entropy of the crystal lattice ΔS_{LAT} was not taken into account. Fig. 3 demonstrates the temperature behavior of the lattice $S_{LAT}(T) - S_{LAT}(100 \text{ K}) = \int_{100}^T (C_{LAT}/T) dT$ and total $S = \int_{100}^T (C_p/T) dT$ entropies in the vicinities of T_1 and T_2 . Temperature dependencies $S(T)$ under pressure were determined by summation of the lattice entropy S_{LAT} and the anomalous contributions ΔS_1 and ΔS_2 shifted along the temperature scale in accordance with the sign of baric coefficients dT_1/dp and dT_2/dp . The values and behavior of extensive BCE, ΔS_{BCE} , at
 110 different pressure were determined from temperature dependencies of the total

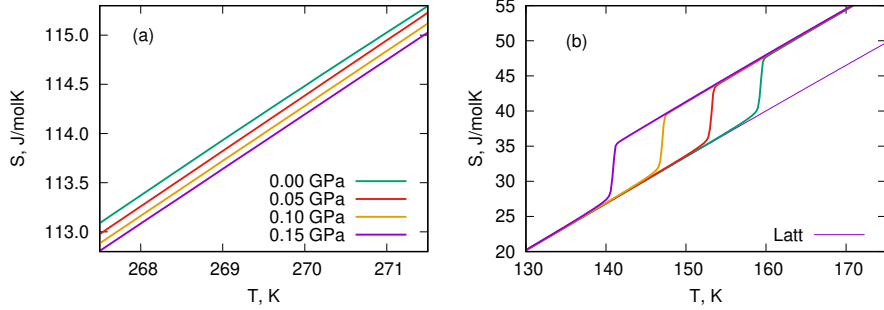


Figure 3: Temperature dependencies of total entropy of NH_4HSO_4 at different hydrostatic pressure near (a) T_1 and (b) T_2 .

entropy as a difference $\Delta S_{BCE} = S(T, p) - S(T, p = 0)$ at constant temperature (Fig. 4(a)). The temperature dependencies of the intensive BCE were revealed analyzing plots of $S(T, p) = S_{LAT}(T, p = 0) + \Delta S(T, p)$ at constant entropy $S(T, p) = S(T + \Delta T_{AD}, p = 0)$ (Fig. 4(b)). Large difference in BCE at T_1 and T_2 at the same pressure is the result of the different values of ΔS_1 and ΔS_2 .

It is known [22] that if we neglect the contribution of the thermal expansion of the crystal lattice, the maximum values of both BCE are limited by the value of the entropy of the phase transition: $(\Delta S_{BCE}^{max})_{T_1} = \Delta S_1 = -10 \text{ J/kg}\cdot\text{K}$, $(\Delta T_{AD}^{max})_{T_1} = 2 \text{ K}$; $(\Delta S_{BCE}^{max})_{T_2} = \Delta S_2 = 68 \text{ J/kg}\cdot\text{K}$, $(\Delta T_{AD}^{max})_{T_2} = 12 \text{ K}$. However, undoubtedly important is the ability to realize in the material maximum values of both BCE at low pressure.

Estimates made using the following relation $p_{min} = T\Delta S / (C_{LAT}dT/dp)$, valid for phase transitions of the first order [9], show that the value $(\Delta S_{BCE}^{max})_{T_2}$ can be implemented in NH_4HSO_4 by rather insignificant pressure 0.1 GPa. In fact, the rather large value $(\Delta S_{BCE})_{T_2} = 0.95(\Delta S_{BCE}^{max})_{T_2}$ can be achieved even at much lower pressure, $p \approx 0.02 \text{ GPa}$ (Fig. 4(a)). However, intensive BCE, which also depends on the dS_{LAT}/dT derivative, is characterized by lower increase rate under pressure and reaches $(\Delta T_{AD}^{max})_{T_2}$ at about 0.13 GPa (Fig. 4(b)). As to the second order phase transition, at pressure 0.1 GPa extensive and intensive effects reach only about 18% of $(\Delta S_{BCE}^{max})_{T_1}$ and $(\Delta T_{AD}^{max})_{T_1}$.

At the second stage, effect of the lattice entropy change under pressure

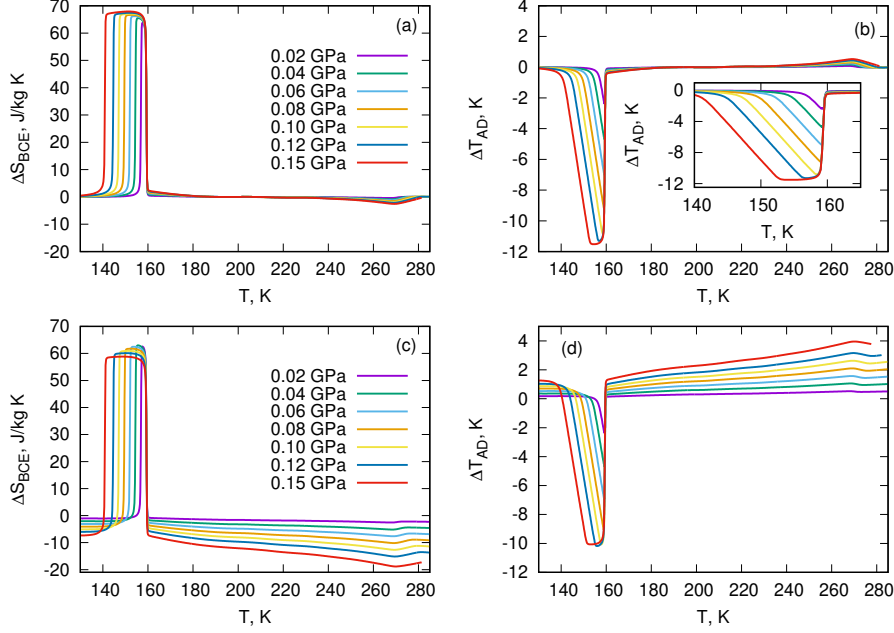


Figure 4: (a) Barocaloric entropy and (b) adiabatic temperature changes at different hydrostatic pressure in a wide temperature range determined without taking into account the effect of thermal expansion of the crystal lattice. Effect of thermal expansion of the crystal lattice on (c) ΔS_{BCE} and (d) ΔT_{AD}

on BCE in NH_4HSO_4 was studied. This contribution can be evaluated using Maxwell relation $(\partial S_{LAT}/\partial p)_T = -(\partial V/\partial T)_p$

$$\Delta S_{LAT}(T, p) = - \int_0^p (\partial V/\partial T)_p dp \approx -V_m \beta_{LAT}(T)p. \quad (2)$$

Here $V_m = 6.17 \times 10^{-5} \text{ m}^3/\text{mol}$ is the molar volume.

Taken into account the data of the thermal expansion study of the related $(\text{NH}_4)_2\text{SO}_4$ [15], it was suggested that the values of β_{LAT} and V_m of NH_4HSO_4 are also weakly depend on the pressure. Lattice contribution was determined
 135 from the results of dilatometric study of NH_4HSO_4 [19].

Fig. 4(c) and (d) demonstrate that due to the same sign of both derivatives, $(\partial V/\partial T)_{T1}$ and $(\partial V_{LAT}/\partial T)$, there is a strong increase in BCE_{conv} . At $p=0.15 \text{ GPa}$, the values $(\Delta S_{BCE})_{T1} = -18.8 \pm 1.5 \text{ J/kg}\cdot\text{K}$ and $(\Delta T_{AD})_{T1} = 4.0 \pm 0.2 \text{ K}$ are about one and a half times higher than even the maximum

140 values considered above as associated with the phase transition entropy ΔS_1 .
 Thus, contributions of $(\Delta S_{BCE}^{LAT})_{T_1}$ and $(\Delta T_{AD}^{LAT})_{T_1}$ to the full BCE at T_1 are
 predominant.

On the other hand, at the same pressure, BCE_{inv} associated with the phase
 transition $Pc-P1$ ($(\partial V/\partial T)_{T_2} < 0$), is reduced to the magnitudes $(\Delta S_{BCE})_{T_2} =$
 145 59 ± 5 J/kg·K, $(\Delta T_{AD})_{T_2} = -10.0 \pm 0.8$ K by BCE_{conv}^{LAT} arising in accordance
 with Eq. 2, $(\partial V_{LAT}/\partial T) > 0$: $(\Delta S_{BCE}^{LAT})_{T_2} = -9.0 \pm 0.7$ J/kg·K, $(\Delta T_{AD}^{LAT})_{T_2} =$
 1.5 ± 0.1 K.

At last, at the third stage, we determine the behavior of extensive and in-
 tensive BCE at T_2 taken into account the peculiarities of experiments with
 150 DTA under pressure. As it was discussed above, increase in pressure strongly
 decreases the entropy jump δS_2 at the first order phase transition $Pc - P1$
 (Fig. 2(b) and (d)), while the total entropy change ΔS_2 remains constant. Ana-
 lyzing the dependencies $S(T, p)$ using both the DTA data under pressure and the
 effect of the lattice expansion, barocaloric parameters at T_2 are determined and
 155 presented in Fig. 5 in comparison with the data obtained in the second stage.
 One can see that in this case the magnitudes of $(\Delta S_{BCE}^{max})_{T_2}$ and $(\Delta T_{AD}^{max})_{T_2}$ are
 realized at almost the same low pressure which was determined in the second
 stage (Fig. 4(c) and (d)). The main difference was observed in the form of peaks
 $(\Delta S_{BCE})_{T_2}(T)$ and $(\Delta T_{AD})_{T_2}(T)$ which is due to peculiarities of the processes
 160 of measuring the heat capacity by methods of adiabatic calorimeter and DTA.

Returning to the results of the BCE study at T_1 , one can confidently ar-
 gue that it would be interesting and useful to investigate the influence of the
 thermal expansion of the crystal lattice on conventional BCE in ferroelectrics
 characterized by large β_{LAT} and undergoing order–disorder transformation with
 165 the positive baric coefficient.

4. Conclusion

This paper demonstrates BCE in NH_4HSO_4 undergoing two successive ferro-
 electric phase transitions characterized by significantly different entropy changes

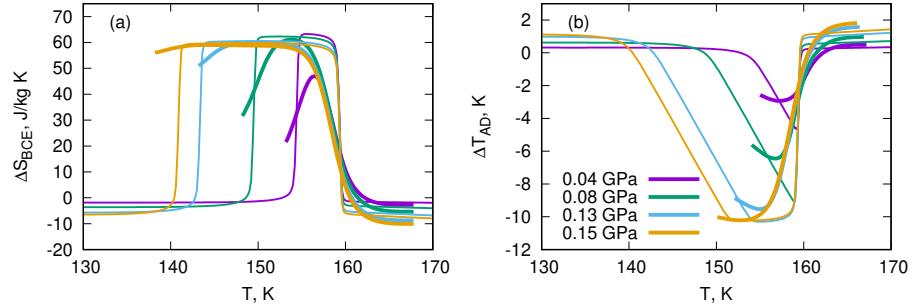


Figure 5: (a) Barocaloric entropy and (b) adiabatic temperature changes at different hydrostatic pressure determined using DTA data on a jump of the entropy (thick lines) and data presented in Fig. 4(c) and (d) (thin lines).

($\Delta S_1=1.2$ J/mol·K, $\Delta S_2=7.6$ J/mol·K) and large baric coefficients of different
 170 sign ($dT_1/dp=+90$ K/GPa and $dT_2/dp=-123$ K/GPa). Hydrostatic pressure
 strongly decreases the entropy jump at T_2 which reaches zero at a pressure of
 0.17 GPa. Very low pressure is needed to realize the maximum values of the
 extensive and intensive inverse BCE. Large thermal expansion of the crystal lat-
 tice leads to two very important points. Firstly, the conventional BCE can be
 175 greatly increased to values much higher than the magnitudes, corresponding to
 the entropy of the phase transition. Secondly, in the case of the negative baric
 coefficient, a conversion from the inverse to conventional BCE can be realized
 by low pressure in the narrow temperature range.

References

180 References

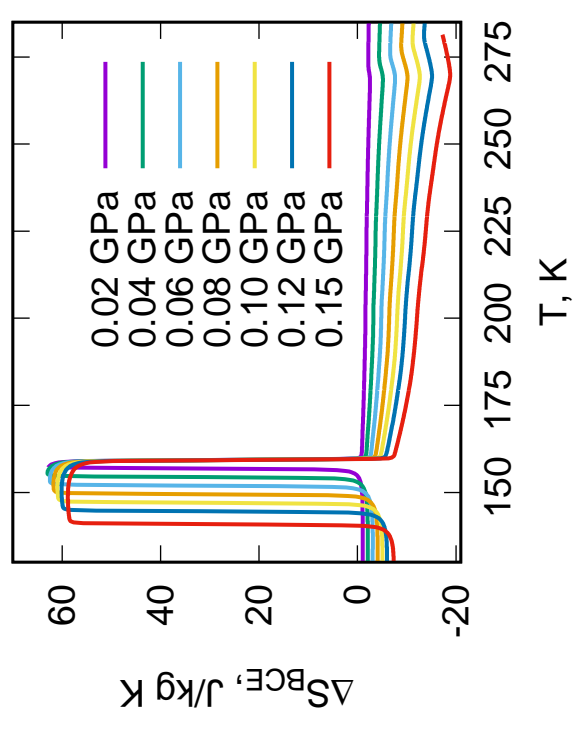
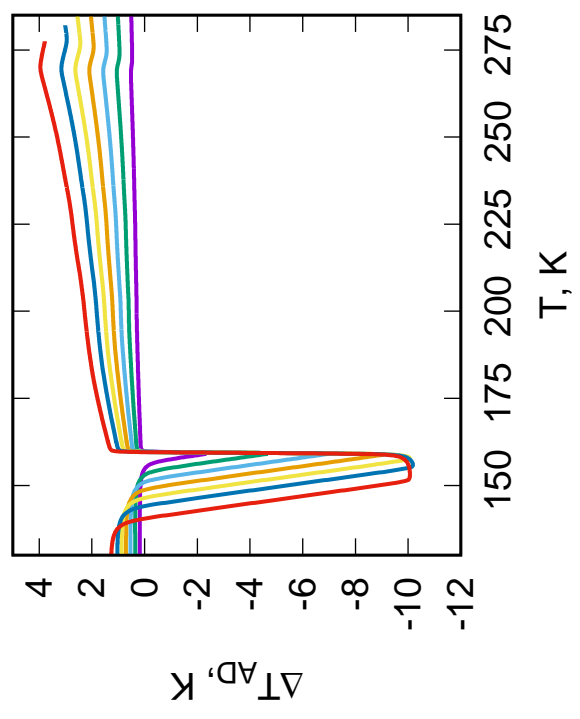
- [1] K. A. Gschneidner Jr, V. K. Pecharsky, A. O. Tsokol, Recent developments
 in magnetocaloric materials, Rep. Prog. Phys. 68 (6) (2005) 1479–1539
 (2005). doi:10.1088/0034-4885/68/6/r04.
- [2] M. Valant, Electrocaloric materials for future solid-state refrigeration tech-
 185 nologies, Prog. Mater. Sci. 57 (6) (2012) 980 – 1009 (2012). doi:10.1016/
 j.pmatsci.2012.02.001.

- [3] X. Moya, S. Kar-Narayan, N. D. Mathur, Caloric materials near ferroic phase transitions, *Nat. Mater.* 13 (2014) 439–450 (2014). doi:10.1038/nmat3951.
- 190 [4] H. Khassaf, T. Patel, R. J. Hebert, S. P. Alpay, Flexocaloric response of epitaxial ferroelectric films, *J. Appl. Phys.* 123 (2) (2018) 024102 (2018). doi:10.1063/1.5009121.
- [5] U. Tomc, J. Tušek, A. Kitanovski, A. Poredoš, A new magnetocaloric refrigeration principle with solid-state thermoelectric thermal diodes, *Appl. Thermal Engineering* 58 (1) (2013) 1–10 (2013). doi:10.1016/j.applthermaleng.2013.03.063.
- 195 [6] U. Plaznik, M. Vrabelj, Z. Kutnjak, B. Malič, A. Poredoš, A. Kitanovski, Electrocaloric cooling: The importance of electric-energy recovery and heat regeneration, *EPL (Europhysics Letters)* 111 (5) (2015) 57009 (2015). doi:10.1209/0295-5075/111/57009.
- 200 [7] A. Kitanovski, U. Plaznik, U. Tomc, A. Poredoš, Present and future caloric refrigeration and heat-pump technologies, *Int. J. Refrigeration* 57 (2015) 288 – 298 (2015). doi:10.1016/j.ijrefrig.2015.06.008.
- [8] N. Michaelis, F. Welsch, S.-M. Kirsch, M. Schmidt, S. Seelecke, A. Schütze, *Experimental parameter identification for elastocaloric air cooling*, *Int. J. Refrigeration* 100 (2019) 167 – 174 (2019). doi:10.1016/j.ijrefrig.2019.01.006.
- 205 [9] M. Gorev, E. Bogdanov, I. Flerov, T-p phase diagrams and the barocaloric effect in materials with successive phase transitions, *J. Phys. D: Appl. Phys.* 50 (38) (2017) 384002 (2017). doi:10.1088/1361-6463/aa8025.
- 210 [10] M. Gorev, E. Bogdanov, I. Flerov, Conventional and inverse barocaloric effects around triple points in ferroelastics $(\text{NH}_4)_3\text{NbOF}_6$ and $(\text{NH}_4)_3\text{TiOF}_5$, *Scripta Materialia* 139 (2017) 53–57 (2017). doi:10.1016/j.scriptamat.2017.06.022.

- 215 [11] E. Mikhaleva, I. Flerov, A. Kartashev, M. Gorev, A. Cherepakhin, K. Sablina, N. Mikhashenok, N. Volkov, A. Shabanov, Caloric effects and phase transitions in ferromagnetic-ferroelectric composites $x\text{La}_{0.7}\text{Pb}_{0.3}\text{MnO}_3-(1-x)\text{PbTiO}_3$, *J. Mater. Res.* 28 (24) (2013) 3322–3331 (2013). doi:10.1557/jmr.2013.360.
- 220 [12] K. Alex Müller, F. Fauth, S. Fischer, M. Koch, A. Furrer, P. Lacorre, Cooling by adiabatic pressure application in $\text{Pr}_{1-x}\text{La}_x\text{NiO}_3$, *Appl. Phys. Letters* 73 (8) (1998) 1056–1058 (1998). doi:10.1063/1.122083.
- [13] T. Strässle, A. Furrer, Z. Hossain, C. Geibel, Magnetic cooling by the application of external pressure in rare-earth compounds, *Phys. Rev. B* 67 (2003) 054407 (2003). doi:10.1103/PhysRevB.67.054407.
- 225 [14] N. A. de Oliveira, Barocaloric effect and the pressure induced solid state refrigerator, *J. Appl. Phys.* 109 (5) (2011) 053515 (2011). doi:10.1063/1.3556740.
- [15] P. Lloveras, E. Stern-Taulats, M. Barrio, J.-L. Tamarit, S. Crossley, W. Li, 230 V. Pomjakushin, A. Planes, L. Manosa, N. D. Mathur, X. Moya, Giant barocaloric effects at low pressure in ferroelectric ammonium sulphate, *Nat. Commun.* 6 (2015) 8801 (2015). doi:10.1038/ncomms9801.
- [16] H. Khassaf, T. Patel, S. P. Alpay, Combined intrinsic elastocaloric and electrocaloric properties of ferroelectrics, *J. Appl. Phys.* 121 (14) (2017) 144102 (2017). doi:10.1063/1.4980098.
- 235 [17] Y. Liu, J. Wei, P.-E. Janolin, I. C. Infante, X. Lou, B. Dkhil, Giant room-temperature barocaloric effect and pressure-mediated electrocaloric effect in BaTiO_3 single crystal, *Appl. Phys. Letters* 104 (16) (2014) 162904 (2014). doi:10.1063/1.4873162.
- 240 [18] M. V. Gorev, I. N. Flerov, E. V. Bogdanov, V. N. Voronov, N. M. Laptash, Barocaloric effect near the structural phase transition in the $\text{Rb}_2\text{KTiOF}_5$

oxyfluoride, *Phys. Solid State* 52 (2) (2010) 377–383 (2010). doi:10.1134/S1063783410020253.

- [19] E. Mikhaleva, I. Flerov, A. Kartashev, M. Gorev, E. Bogdanov, V. Bondarev, Thermal, dielectric and barocaloric properties of NH_4HSO_4 crystallized from an aqueous solution and the melt, *Solid State Sciences* 67 (2017) 1–7 (2017). doi:10.1016/j.solidstatesciences.2017.03.004.
- [20] R. Pepinsky, K. Vedam, S. Hoshino, Y. Okaya, Ammonium hydrogen sulfate: A new ferroelectric with low coercive field, *Phys. Rev.* 111 (1958) 1508–1510 (1958). doi:10.1103/PhysRev.111.1508.
- [21] D. Swain, V. S. Bhadram, P. Chowdhury, C. Narayana, Raman and x-ray investigations of ferroelectric phase transition in NH_4HSO_4 , *J. Phys. Chem. A* 116 (2012) 223–230 (2012). doi:10.1021/jp2075868.
- [22] R. Pirc, Z. Kutnjak, R. Blinc, Q. M. Zhang, Upper bounds on the electrocaloric effect in polar solids, *Appl. Phys. Letters* 98 (2) (2011) 021909 (2011). doi:10.1063/1.3543628.



- Temperature/entropy – pressure phase diagrams of ferroelectric NH_4HSO_4 were studied
- Pressure strongly effects on the temperature and entropy of the phase transitions.
- Low pressure induces large inverse barocaloric effect at first order transformation.
- Expansion of the crystal lattice strongly affects the barocaloric efficiency.
- The conversion between the inverse and conventional barocaloric effects is found.

LaTeX Source Files

[Click here to download LaTeX Source Files: manuscript_rev.zip](#)

LaTeX Source Files

[Click here to download LaTeX Source Files: manuscript_BCE_AHS.zip](#)

LaTeX Source Files

[Click here to download LaTeX Source Files: manuscript_rev2 \(1\).zip](#)